



This discussion paper is/has been under review for the journal Atmospheric Chemistry and Physics (ACP). Please refer to the corresponding final paper in ACP if available.

Iodine chemistry in the troposphere and its effect on ozone

A. Saiz-Lopez¹, R. P. Fernandez^{1,*}, C. Ordóñez², D. E. Kinnison³,
J. C. Gómez Martín^{1,**}, J.-F. Lamarque³, and S. Tilmes³

¹Atmospheric Chemistry and Climate Group, Institute of Physical Chemistry Rocasolano, CSIC, Madrid 28006, Spain

²Met Office, EX1 3PB, Exeter, UK

³Atmospheric Chemistry Division, NCAR, Boulder, CO 80301, USA

*now at: National Research Council (CONICET), UTN-FRM, ICB-UNCuyo, Mendoza 5501, Argentina

**now at: School of Chemistry, University of Leeds, LS2 9JT, Leeds, UK

Received: 10 July 2014 – Accepted: 19 July 2014 – Published: 1 August 2014

Correspondence to: A. Saiz-Lopez (a.saiz@csic.es)

Published by Copernicus Publications on behalf of the European Geosciences Union.

Title Page

Abstract

Introduction

Conclusions

References

Tables

Figures



Back

Close

Full Screen / Esc

Printer-friendly Version

Interactive Discussion



Abstract

Despite potential influence of iodine chemistry on the oxidizing capacity of the troposphere, reactive iodine distributions and their impact on tropospheric ozone remain nearly unexplored aspects of the global atmosphere. Here we present a comprehensive global modelling experiment aimed at estimating lower and upper limits of the inorganic iodine burden and its impact on tropospheric ozone. Two sets of simulations without and with the photolysis of I_xO_y oxides (i.e., I_2O_2 , I_2O_3 and I_2O_4) were conducted to define the range of inorganic iodine loading, partitioning and impact in the troposphere. Our results show that the most abundant daytime iodine species throughout the middle to upper troposphere is atomic iodine, with an annual average tropical abundance of (0.15–0.55) pptv. We propose the existence of a “tropical ring of atomic iodine” that peaks in the tropical upper troposphere (~ 11 – 14 km) at the Equator and extends to the sub-tropics (30° N– 30° S). Annual average daytime I/IO ratios larger than 3 are modelled within the tropics, reaching ratios up to ~ 20 during vigorous uplift events within strong convective regions. We calculate that the integrated contribution of catalytic iodine reactions to the total rate of tropospheric ozone loss ($IO_{x_{Loss}}$) is 2–5 times larger than the combined bromine and chlorine cycles. $IO_{x_{Loss}}$ cycles, without and with I_xO_y photolysis, represent approximately (17–27)%, (8–14)% and (11–27)% of the tropical annual ozone loss for the marine boundary layer (MBL), free troposphere (FT) and upper troposphere (UT), respectively. Our results indicate that iodine is the second strongest ozone depleting family throughout the global marine UT and in the tropical MBL. We suggest (i) iodine sources and its chemistry need to be included in global tropospheric chemistry models, (ii) experimental programs designed to quantify the iodine budget in the troposphere should include a strategy for the measurement of atomic I, and (iii) laboratory programs are needed to characterize the photochemistry of higher iodine oxides to determine their atmospheric fate since they can potentially dominate halogen-catalysed ozone destruction in the troposphere.

Iodine chemistry in the troposphere and its effect on ozone

A. Saiz-Lopez et al.

Title Page

Abstract

Introduction

Conclusions

References

Tables

Figures



Back

Close

Full Screen / Esc

Printer-friendly Version

Interactive Discussion



1 Introduction

The oceans provide the main source of iodine to the atmosphere. Methyl iodide (CH_3I) and other very short-lived (VSL) iodocarbons (e.g. CH_2I_2 , $\text{C}_2\text{H}_5\text{I}$, $\text{C}_3\text{H}_7\text{I}$, CH_2ICl , CH_2IBr) are produced by biotic and photochemical processes, and released to the atmosphere from supersaturated ocean waters (Carpenter et al., 2012; Saiz-Lopez et al., 2012a). Laboratory studies have also established the gaseous emission of molecular iodine (I_2) following the reaction of aqueous iodide with atmospheric ozone at the sea surface (Garland and Curtis, 1981; Sakamoto et al., 2009; Hayase et al., 2010). More recently, it has been shown that HOI is the major species emitted as a result of this oxidative reaction (Carpenter et al., 2013; MacDonald et al., 2014). Several modeling studies and analysis of experimental data have suggested that the HOI/ I_2 additional inorganic source must surpass the emission strength of organic VSL iodocarbons in order to reproduce observed iodine monoxide (IO) measurements over the open ocean environment (Jones et al., 2010; Mahajan et al., 2010, 2012; Gómez Martín et al., 2013b; Großmann et al., 2013; Lawler et al., 2014).

Early pioneering work by Chameides and Davis (1980) and Solomon et al. (1994) showed that both organic and inorganic iodine compounds photo-dissociate rapidly in the troposphere to release iodine atoms, which then react mainly with ozone to generate IO. A steady state is then established between I and IO as a result of the fast photolysis of the oxide, and therefore the two species are termed collectively as reactive iodine, or $\text{IO}_x = \text{I} + \text{IO}$. IO_x react further with other species to generate different forms of inorganic iodine (Saiz-Lopez et al., 2012a, see Table 1). The atmospheric chemical processing of iodine species influences the oxidizing capacity of the troposphere through catalytic ozone depleting cycles ($\text{IO}_{x\text{Loss}}$, i.e. Brasseur and Solomon, 2006; Chameides and Davis, 1980; McFiggans et al., 2000; Solomon et al., 1994; Vogt et al., 1999) and changes to the HO_x (i.e., $[\text{HO}_2]/[\text{OH}]$) and NO_x (i.e., $[\text{NO}_2]/[\text{NO}]$) ratios (Bloss et al., 2005). It also makes a negative contribution to the radiative flux in the tropical troposphere (Saiz-Lopez et al., 2012b), and produces higher order iodine

Title Page

Abstract

Introduction

Conclusions

References

Tables

Figures



Back

Close

Full Screen / Esc

Printer-friendly Version

Interactive Discussion



oxides (I_xO_y) which have been proposed to participate in the formation of ultrafine aerosol particles in coastal environments (Hoffmann et al., 2001; O'Dowd et al., 2002; Jimenez et al., 2003; McFiggans et al., 2004, 2010; Pechtl et al., 2006; Saiz-Lopez et al., 2006; Huang et al., 2010; Mahajan et al., 2011; Atkinson et al., 2012).

Different techniques have enabled measurements of tropospheric iodine species in geographical locations ranging from the tropical troposphere to the polar boundary layer (Saiz-Lopez and von Glasow, 2012). Comprehensive reports and inventories of organic VSL iodocarbons across the world oceans have been published in the last decades (Saiz-Lopez et al., 2012a, and references therein). Inorganic reactive iodine species have been observed in the marine boundary layer (MBL) well above their detection limits, including IO (Alicke et al., 1999), OIO (Allan et al., 2000), I_2 (Saiz-Lopez and Plane, 2004), and I (Bale et al., 2008). More recently, the detection of IO in the subtropical (Puentedura et al., 2012) and tropical (Dix et al., 2013) free troposphere shows a widespread presence of active iodine species throughout the marine troposphere.

Photochemical (Solomon et al., 1994; Vogt et al., 1999; Calvert and Lindberg, 2004; Saiz-Lopez et al., 2007; Sommariva and von Glasow, 2012; Sommariva et al., 2012) and global (Saiz-Lopez et al., 2012b) modeling studies have suggested the potential important role of iodine in the tropospheric ozone burden based on its faster catalytic ozone-depletion kinetics compared to that of bromine and chlorine. Additionally, recent studies have pointed out differences between ozonesonde climatologies and modeled O_3 abundances in the upper tropical troposphere (Young et al., 2013) and northern mid-latitude lower troposphere (Parrish et al., 2014), and highlighted the importance of performing a rigorous investigation of additional factors driving the budget of tropospheric ozone. Following the evidence of the ubiquitous presence of reactive iodine in the troposphere, we present simulations with a chemistry-climate model that includes geographically distributed VSL iodocarbon sources (CH_3I , CH_2I_2 , CH_2ICl and CH_2IBr) as well as global inorganic iodine emissions (HOI/I_2) from the oceans. The model includes a state-of-the-art iodine chemistry scheme considering I_xO_y and their photolytic and thermal decomposition, individualized wet-removal processes and ice-uptake, as

Iodine chemistry in the troposphere and its effect on ozone

A. Saiz-Lopez et al.

Title Page

Abstract

Introduction

Conclusions

References

Tables

Figures



Back

Close

Full Screen / Esc

Printer-friendly Version

Interactive Discussion



can be directly addressed. See Lamarque et al. (2012) for a complete description of the SD setup.

The development of the benchmark CAM-Chem mechanism is based on MOZART-4 (Emmons et al., 2010). For this configuration, an improved representation of stratospheric chemistry, considering heterogeneous processes in polar clouds from MOZART-3 (Kinnison et al., 2007; Wegner et al., 2013) has also been used. The chemical solver is initialized with identical chemical boundary conditions for any given species in all simulations presented here, and all the atmospheric oxidants are computed online at all times (i.e., without considering prescribed monthly OH fields as done in previous studies). Our current setup includes an organic and inorganic halogen (chlorine, bromine and iodine) photochemistry mechanism, considering both natural and anthropogenic sources, heterogeneous recycling, dry and wet deposition; both in the troposphere and lower stratosphere (Ordóñez et al., 2012; Fernandez et al., 2014). For iodine species we have compiled a state-of-the-art chemical scheme as described below.

2.1 Atmospheric chemistry of iodine

The chemistry of chlorine and bromine VSL species in CAM-Chem has been described in detail previously (Ordóñez et al., 2012; Fernandez et al., 2014). In this work we have used the same emissions inventory of bromo- (CHBr_3 , CH_2Br_2 , CH_2BrCl , CHBr_2Cl and CHBrCl_2) and iodo- carbons presented there, extending the iodine inorganic chemistry mechanism. VSL oceanic sources of CH_2I_2 , CH_2ICl and CH_2IBr are based on parameterizations of chlorophyll *a* satellite maps, including latitudinal variations between 50°N – 50°S and an annual seasonality. The global CH_2IX (with $X = \text{Cl}, \text{Br}$ or I) flux in the model is $\sim 437 \text{ Gg yr}^{-1}$. CH_3I emissions are taken from an existing top-down inventory (Bell et al., 2002), which included major oceanic sources (213 Gg yr^{-1}) as well as some land-based fluxes from rice paddies, wetlands, biofuel and biomass burning (91 Gg yr^{-1}), yielding a global CH_3I flux of 304 Gg yr^{-1} . For the emissions of most VSL

Iodine chemistry in the troposphere and its effect on ozone

A. Saiz-Lopez et al.

Title Page

Abstract

Introduction

Conclusions

References

Tables

Figures



Back

Close

Full Screen / Esc

Printer-friendly Version

Interactive Discussion



Iodine chemistry in the troposphere and its effect on ozone

A. Saiz-Lopez et al.

Title Page

Abstract

Introduction

Conclusions

References

Tables

Figures



Back

Close

Full Screen / Esc

Printer-friendly Version

Interactive Discussion



iodocarbons we follow a solar diurnal profile, with emissions peak in the early afternoon and null emissions at night. The exception is CH_2I_2 which showed an improved agreement with measurements when $\sim 1/4$ of the total emissions occurs during the night (Ordóñez et al., 2012). In addition, inorganic iodine oceanic sources have been included in the model, based on recent laboratory studies that determined the abiotic gaseous emission of HOI and I_2 following the oxidation of aqueous iodide by atmospheric ozone (Carpenter et al., 2013; MacDonald et al., 2014). The global modelled emissions of HOI/ I_2 account for $\sim 1.9 \text{ Tg (I) yr}^{-1}$ and depend on the deposition of tropospheric ozone to the ocean surface, the sea surface temperature and the wind speed. The computed lifetimes of CH_2ICl , CH_2IBr and CH_2I_2 range from minutes to hours in agreement with previous studies (Rattigan et al., 1997; Roehl et al., 1997; Mössinger et al., 1998), while for CH_3I it is in the order of 5–8 days (Rattigan et al., 1997; Roehl et al., 1997).

Table 1 presents the bimolecular, thermal decomposition and termolecular reactions of iodine species included in the chemical mechanism. Updates with respect to previous analyses (Ordóñez et al., 2012; Saiz-Lopez et al., 2012b) are mainly based on theoretical studies on the formation, photochemistry and thermal decomposition of higher iodine oxides, collectively called I_xO_y (Gómez Martín et al., 2007; Kaltsoyannis and Plane, 2008; Gómez Martín and Plane, 2009). A distinct feature of iodine chemistry, with respect to the other halogens, is the formation of I_xO_y (where usually $x = 2$ and $y = 2, 3$, or 4) from recombination reactions of IO with itself ($y = 2$) and with OIO ($y = 3$), or OIO with itself ($y = 4$). Unambiguous discriminated observation of I_xO_y has been achieved only recently by means of photo-ionisation time-of-flight mass spectrometry (Gómez Martín et al., 2013a). This recent work also confirmed the minor role played by ozone in the formation of iodine aerosol (Saunders et al., 2010), which rules out I_2O_5 as nucleating species (Saunders and Plane, 2005). Some other iodine oxides with different I/O stoichiometry ($x \neq 2$) have been suggested to participate in complex mechanisms of particle formation (Gálvez et al., 2013; Gómez Martín et al., 2013a),

Iodine chemistry in the troposphere and its effect on ozone

A. Saiz-Lopez et al.

Title Page

Abstract

Introduction

Conclusions

References

Tables

Figures



Back

Close

Full Screen / Esc

Printer-friendly Version

Interactive Discussion



under the IO spectrum to a single species (I_2O_2), Gómez Martín et al. (2005, 2007) obtained evidence of the same band resulting from an overlap of at least two different iodine oxides (I_2O_2 and I_2O_3). Here, in order to calculate atmospheric photolysis rates, we adopt for these two species the spectra extracted and scaled to absolute absorption cross section by Gómez Martín et al. (2005) (Fig. 1). Extraction of the I_2O_4 absorption spectrum from the observed I_xO_y broadband absorption was unfeasible, and therefore, in the present work, a solution spectrum measured at the University of Leeds has been used. The I_2O_4 spectrum was measured at 1 nm resolution using a Perkin-Elmer Lambda 900 UV-Vis spectrometer in a 1 cm quartz cuvette (R. Saunders, personal communication, 2011). I_2O_4 was synthesized from commercial I_2O_5/I_2 and H_2SO_4 (Sigma Aldrich). This made iodosyl sulphate, which then, washed, converted to I_2O_4 (Daehlie and Kjekshus, 1964).

2.3 Model simulations

Total inorganic iodine (I_y) has been defined as:

$$I_y = I + IO + HOI + IONO_2 + I_xO_y + I_{\text{minor}} + I_{\text{dihal}} \quad (1)$$

where for simplicity

$$I_xO_y = 2 \times (I_2O_2 + I_2O_3 + I_2O_4) \quad (2)$$

$$I_{\text{minor}} = HI + OIO + INO_2 + INO \quad (3)$$

$$I_{\text{dihal}} = 2 \times I_2 + IBr + ICl \quad (4)$$

Two independent simulations were performed in order to estimate the range of I_y loading and impact in the troposphere: the *Base* scheme and the $J_{I_xO_y}$ scheme. The *Base* scheme does not consider the photolysis of I_xO_y oxides (i.e., I_2O_2 , I_2O_3 and I_2O_4) and represents the lower I_y loading limit. In this simulation I_xO_y are decomposed back to IO_x only by thermal decomposition, being removed from the gas phase via

washout, uptake on sea-salt aerosols and dry deposition processes. The $J_{I_xO_y}$ scheme includes, in addition, the photolysis of I_xO_y , allowing for an efficient recycling of IO_x in the gas phase within the troposphere. Therefore this second simulation represents the upper limit of tropospheric I_y loading. Hereafter we use these two simulations to provide a range of reactive iodine loading, partitioning and distributions throughout the troposphere consistent with our current knowledge of iodine chemistry (within its uncertainties).

3 Results and discussions

The upper and lower limits of total inorganic iodine loading in the troposphere have been estimated by conducting simulations where the photolysis of I_xO_y was allowed ($J_{I_xO_y}$) or neglected (*Base*), respectively. The last of a 3 year simulation was used to compute the iodine atmospheric burden for both cases. As the model is configured with prescribed sea surface temperatures (SST) and ice-coverage for the 2000 decade (Rayner, 2003), results are not representative of the meteorology of any specific year, and annual averages are presented unless specifically mentioned. Three different vertical regions on consecutive non-overlapping altitude intervals were defined within the tropics (20° N– 20° S) and mid-latitudes (50° N– 20° N and 20° S– 50° S): MBL, expanding from the ocean surface up to ~ 900 m a.s.l. (~ 900 hPa); the FT, from ~ 900 m (900 hPa) to ~ 8.5 km (~ 350 hPa); and the UT from ~ 8.5 km (~ 350 hPa) up to the model tropopause. Besides the standard 24 h averaged streaming, time dependent volume mixing ratios (vmr) for day and night has been generated considering the noon (11:30–12:30) and midnight (23:30–00:30) local time, respectively, for all latitudes and longitudes.

Iodine chemistry in the troposphere and its effect on ozone

A. Saiz-Lopez et al.

Title Page

Abstract

Introduction

Conclusions

References

Tables

Figures



Back

Close

Full Screen / Esc

Printer-friendly Version

Interactive Discussion



3.1 The partitioning of VSL iodine source gases

Figure 2 shows the vertical profiles of the four major VSL iodocarbons together with their photochemical decomposition rates within the tropics. On an annual average, the total organic iodine abundance results in ~ 0.8 pptv in the MBL and ~ 0.1 pptv in the FT (Fig. 2a). The percentage contribution of each individual VSL species to total organic iodine is approximately 82 % (96 %), 12 % (2.7 %), 5 % (0.8) and 1 % (0.1 %) for CH_3I , CH_2I_2 , CH_2I_2 and CH_2IBr in the MBL and (FT), respectively. Iodine-containing di-halocarbons are photolyzed almost entirely within the MBL, and the predominant organic species in the free troposphere is methyl iodide. As a consequence, CH_3I is the only iodocarbon reaching the lower tropical tropopause layer (TTL) by efficient convection, although integrated in the tropics it represents a negligible ($\sim 10^{-3}$ pptv) carbon-bonded residual at the coldest point tropopause ($\theta_{\text{cpt}} \approx 380$ K, approx. at 17 km) in agreement with previous studies that determined an inconsiderable injection of VSL iodocarbons into the stratosphere (Montzka et al., 2011; Tegtmeier et al., 2013).

Even when the added photodecomposition of CH_2I_2 , CH_2IBr and CH_2I_2 within the MBL represents an additional source of inorganic iodine comparable to that of CH_3I (Fig. 2b), several studies have suggested that an additional source of active iodine must exist at the sea-surface in order to reconcile open ocean measurements of IO with current knowledge of iodine sources and chemistry (Jones et al., 2010; Mahajan et al., 2010; Gómez Martín et al., 2013b; Großmann et al., 2013). Within CAM-Chem, the inorganic iodine (HOI/I_2) released from the tropical oceans following the work of Carpenter et al. (2013) and MacDonald et al. (2014) (see red dot in Fig. 2b, $\sim 6.3 \times 10^3 \text{ atoms cm}^{-3} \text{ s}^{-1}$) is an order of magnitude higher than that from all organoiodine species combined ($\sim 5.7 \times 10^2 \text{ atoms cm}^{-3} \text{ s}^{-1}$ at the surface level and totaling $\sim 1.0 \times 10^3 \text{ atoms cm}^{-3} \text{ s}^{-1}$ in the MBL), and is the dominant source of iodine within the MBL. Another important source of reactive iodine in the lower troposphere is the photolysis of the diatomic ICl and IBr species recycled by heterogeneous reactions over sea-salt aerosols (red line in Fig. 2b), which we calculate to be the most important

Iodine chemistry in the troposphere and its effect on ozone

A. Saiz-Lopez et al.

Title Page

Abstract

Introduction

Conclusions

References

Tables

Figures



Back

Close

Full Screen / Esc

Printer-friendly Version

Interactive Discussion



Iodine chemistry in the troposphere and its effect on ozone

A. Saiz-Lopez et al.

Title Page

Abstract

Introduction

Conclusions

References

Tables

Figures



Back

Close

Full Screen / Esc

Printer-friendly Version

Interactive Discussion



process releasing atomic iodine when integrating the first 5 km in the marine atmosphere. Note that the implementation of sea-salt recycling in CAM-Chem for iodine species does not constitute a net source of iodine to the troposphere (see Table 3) but represents only a change in iodine partitioning that slows down the conversion of reactive iodine into reservoir species with greater washout efficiencies (i.e., HOI or IONO₂). The photolysis of CH₃I represents 10 %, 60 % and 83 % of the total iodine sources from VSL photodecomposition within the MBL, FT and UT respectively, whereas in the lower TTL the source of iodine becomes almost solely CH₃I. The other VSL iodocarbon with a non-negligible contribution to I_y in the FT and UT is CH₂ICl, its I atom release can reach 22 % (FT), 10 % (UT) and 5 % (TTL) of the total iodine source. Note that CH₂ICl is the di-halogen iodocarbon with the longest lifetime (~ 8 h) and it represents the strongest oceanic VSL source on an iodine-atom basis (Ordóñez et al., 2012).

The very rapid photolysis of iodocarbons, compared to transport times, makes the relative contribution from each VSL species to the inorganic iodine release to be almost independent on the spatial scale considered. For example, on an annual average, from the total tropical release of atomic iodine at 12 km 90 % arise from CH₃I and 7 % from CH₂ICl, while their respective percentage contributions are 85 % and 10 % within the convective Western Pacific (WP) warm pool during February. This is in contrast to the longer-lived VSL bromocarbons, where the total amount of atomic bromine released from each independent species at a given altitude, within the TTL, strongly depends on the strength of convection (Fernandez et al., 2014). For VSL iodocarbons, the I_y loading in the FT and UT depends mainly on the geographical distribution and intensity of CH₃I oceanic emissions, which presents localized areas with stronger fluxes, such as the Indian Ocean and the WP region. Ordóñez et al. (2012) also found that using an emission cycle with non-zero emissions during the night, the monthly average concentrations of CH₂IX species increase: e.g. the iodocarbons, which are the VSL species with shortest lifetimes, can temporally accumulate in the MBL and be transported to higher altitudes. This highlights the importance of experimentally determining the shape of the diurnal emission profile to estimate the overall impact of VSL iodocarbons at different heights.

3.2 Iodine burden in the troposphere and the role of I_xO_y

The fast reactions $IO + IO$, $IO + OIO$ and $OIO + OIO$ lead to the formation of significant levels of I_2O_2 , I_2O_3 and I_2O_4 , respectively. As within the *Base* scheme only thermal decomposition and deposition onto background aerosol of iodine oxides are allowed, the levels of I_xO_y build up in the atmosphere, reaching a total iodine abundance > 1 pptv in the FT and UT (Fig. 2c). If I_xO_y were not photolabile they would represent 30% of the total I_y abundance in the MBL and more than 70% in the FT and UT. This large mass of iodine in the atmosphere is currently unaccounted for and subject to a large degree of uncertainty about the photochemistry of higher iodine oxides. This presents a fundamental problem in the quantification of iodine chemistry and its effect in the atmosphere, as the particle nucleating I_xO_y species do not release active iodine back to the gaseous phase (especially in the FT and UT where temperatures are too low for thermal decomposition to be efficient), representing an effective sink of atmospheric iodine. As many uncertainties still exist on which are the dominant photochemical processes affecting I_xO_y species, hereafter, we present our best estimate of the upper and lower range of tropospheric iodine loading and its partitioning for the *Base* and $J_{I_xO_y}$ schemes defined in Sect. 2.3. Most likely, an intermediate mechanism between these two scenarios controls the iodine recycling in the real atmosphere, with a portion of the I_xO_y being removed by wet/dry deposition, another one forming larger iodine aggregates which will likely be lost to aerosol, and the rest being recycled to IO_x in the gas phase by photolysis.

Figure 3a shows the range of vertical distribution of the main annually averaged noontime iodine species within the tropics ($20^\circ N$ – $20^\circ S$) for the *Base* and $J_{I_xO_y}$ schemes. From the surface to about 7–8 km HOI is the main daytime iodine reservoir. Above that height, atomic iodine becomes the dominant iodine species during the day from the mid- to upper-troposphere, resulting in an averaged 19% (58%) of the total daytime I_y in the UT for the *Base* and ($J_{I_xO_y}$) schemes, respectively. On an annual average, surface daytime IO mixing ratios over the tropical oceans range from 0.45 to

Iodine chemistry in the troposphere and its effect on ozone

A. Saiz-Lopez et al.

Title Page

Abstract

Introduction

Conclusions

References

Tables

Figures



Back

Close

Full Screen / Esc

Printer-friendly Version

Interactive Discussion



Iodine chemistry in the troposphere and its effect on ozone

A. Saiz-Lopez et al.

Title Page

Abstract

Introduction

Conclusions

References

Tables

Figures

◀

▶

◀

▶

Back

Close

Full Screen / Esc

Printer-friendly Version

Interactive Discussion



0.7 pptv in agreement with recent ship-borne measurements performed over remote open oceans (Mahajan et al., 2012; Großmann et al., 2013). Above the MBL, IO vertical profiles remain in the range (0.1–0.25) pptv between 2 and 8 km, in agreement with recent measurements in the FT performed over the tropical Atlantic (Puentedura et al., 2012) and Pacific (Dix et al., 2013) oceans. The tropospheric IO vertical profiles show two distinct vertical shapes depending on the inclusion or not of the I_xO_y photolysis: (within the *Base* scheme there is an evident reduction of IO concentrations with altitude ($IO^{12km} = 0.04$ pptv) due to the large conversion of IO_x to un-reactive I_xO_y in the UT; while for the $J_{I_xO_y}$ scheme high levels of IO are maintained throughout the FT and up to the UT ($IO^{12km} = 0.16$ pptv), see Sect. 3.4). Dix et al. (2013) reported IO vertical profiles over the Pacific Ocean and suggested the existence of an additional process (which they proposed to be heterogeneous sea-salt recycling) in order to sustain the elevated IO levels observed throughout the mid- and upper-FT. Our modelling results indicate that heterogeneous recycling on sea-salt can contribute to the IO profile up to about 5 km (Fig. 2b), however it is very unlikely that reactions on sea-salt can be a source of iodine towards the upper FT, except within convective regions, due to its negligible number concentration at those heights. Instead, we suggest that the combined release of I atoms from CH_3I photolysis and the photolytic recycling of gaseous I_xO_y within the $J_{I_xO_y}$ scheme can account for the increase in IO_x lifetime required to reconcile our current understanding of iodine chemistry to recent field measurements throughout the mid- to upper-troposphere (Fig. 3a, see also Sect. 3.4).

The comparative release of reactive iodine species due to CH_3I photolysis (defined as $d[I]/dt$) and thermal and photolytic breakdown of I_xO_y (defined as $d[IO_x]/dt$) is shown in Fig. 4. Photochemical decomposition of CH_3I accounts for up to 50 atoms $I\text{ cm}^{-3}\text{ s}^{-1}$, within the MBL, and between 2 and 8 atoms $I\text{ cm}^{-3}\text{ s}^{-1}$ in the tropical FT (Fig. 4a). As *Base* and $J_{I_xO_y}$ schemes consider identical VSL sources, the latitudinal distributions are equivalent for both schemes. Within the *Base* scheme the release of inorganic iodine from VSL sources in the FT is up to 3 orders of magnitude larger than the contribution from I_xO_y thermal decomposition (Fig. 4b), and controls

Iodine chemistry in the troposphere and its effect on ozone

A. Saiz-Lopez et al.

[Title Page](#)[Abstract](#)[Introduction](#)[Conclusions](#)[References](#)[Tables](#)[Figures](#)[Back](#)[Close](#)[Full Screen / Esc](#)[Printer-friendly Version](#)[Interactive Discussion](#)

the tropospheric inorganic iodine burden. Due to the slow thermal breakdown of higher oxides, I_xO_y accumulate in the FT (Fig. 2c, see also Sect. 3.4). When the photolysis of I_xO_y is allowed, this process constitutes the most important source of reactive iodine in the tropical free troposphere, recycling back more than 500 IO_x molecules $cm^{-3} s^{-1}$, and avoiding a large I_xO_y accumulation. As a consequence, larger amounts of IO_x are maintained at higher altitudes (Fig. 3a). It is worth noting that the photodecomposition of CH_3I is the first step providing iodine atoms in the FT, and without the contribution from this organic precursor, the impact of iodine chemistry in the FT and UT would be negligible.

It is worth noting how the crossing-points height for the I-IO (~ 7 km), I-HOI (~ 9 km) and IO-HOI (~ 11 km) vertical noontime profiles occurs at the same altitude, regardless of the consideration or not of the photolysis of the I_xO_y (see Fig. 3a). This confirms that the steady state reached is nearly independent of the total amount of I_y as expected due to the rapid photochemical time constants of the gaseous iodine system. The importance of constraining the absolute I_y loading in the mid- and upper-troposphere is more notorious if we consider that the relative oxidative potential of iodine chemistry is greater in the upper troposphere, and that ~ 80 % of the halogen mediated tropospheric ozone loss occurs above 800 hPa (Saiz-Lopez et al., 2012b, see Sect. 3.5).

During the night, the main reservoir species in the mid- and upper-troposphere is HOI (Fig. 3b), which accounts for 70 % of the total nighttime I_y in the FT for the $J_{I_xO_y}$ scheme. Therefore, HOI is the most abundant iodine species in the lower troposphere both during the day and at night, and its washout efficiency controls the total atmospheric iodine burden. Indeed, the Henry's law constant for HOI (K_H^{HOI}) has been adjusted between a more (*Base*) and less ($J_{I_xO_y}$) efficient value within the range of measurements and uncertainties reported in the literature (Sander, 1999; see also Table 4). Within the $J_{I_xO_y}$ scheme, the $IONO_2$ abundance increases significantly above 10 km, representing the most abundant nighttime inorganic reservoir in the TTL ($IONO_2^{15km} = 0.4$ pptv). In the case of the *Base* scheme, since less IO is available (i.e. due to the irreversible

conversion of IO to I₂O₂ in the cold UT) for reaction with NO₂, the IONO₂ levels in the UT are considerably lower (Fig. 3b), and most of iodine remains in the form of I_xO_y. This implies that once I_xO_y are formed within the *Base* scheme, they do not further release active iodine back to the gas phase, and then behave as an unreactive sink of iodine that accumulates in the gas phase. As during daytime, the nocturnal crossing altitude of the HOI and IONO₂ vertical profiles is equivalent for both schemes (~ 15 km), indicating that the relative partitioning of the main I_y species does not depend on the overall I_xO_y or total I_y abundances.

3.3 The tropical ring of atomic iodine

Levels of daytime atomic I increase significantly in the middle and upper troposphere due to the low ozone concentrations and temperatures prevailing in these regions, which slowdown the formation of IO by the I + O₃ Arrhenius type reaction (Sander et al., 2011). Under these conditions, we simulate a daytime “tropical ring of atomic iodine” with a latitudinal extent from 30° N to 30° S (Fig. 5). Within this tropical ring, annual zonal average atomic I peaks at 0.2 and 0.65 pptv for the *Base* and J_{I_xO_y} schemes, respectively, accounting for up to 70 % of the total annually-averaged I_y in the tropics (black contour lines in Fig. 5). The altitude at which the maximum modeled I atom levels are observed depends on the photochemical scheme considered: for the *Base* scheme the atomic ring extends from 7 to 15 km, peaking at ~ 11 km (Fig. 5a–c), while for the J_{I_xO_y} scheme it expands from 8 to 17 km, with maximum abundances located at ~ 14 km (Fig. 5d–f). The longitudinal (Fig. 5b and e) and temporal (Fig. 5c and f) variation of the atomic iodine tropical ring suggests that atomic I is globally and annually the most abundant daytime iodine species within the tropics from about 9 km up to the tropopause. The highest I atom concentrations within the tropical ring are modeled to exist within regions of strong oceanic sources and during periods of strong convection, when large amounts of inorganic iodine are rapidly transported from the MBL to the FT

Iodine chemistry in the troposphere and its effect on ozone

A. Saiz-Lopez et al.

Title Page

Abstract

Introduction

Conclusions

References

Tables

Figures



Back

Close

Full Screen / Esc

Printer-friendly Version

Interactive Discussion



and UT. For example, within the WP region, the monthly I atom abundance peaks at 0.30 and 0.90 pptv for the *Base* and $J_{I_xO_y}$ schemes, respectively.

In both simulated schemes the atomic tropical ring and the relative I/I_y distributions are coincident in altitude. Note however that the ultimate fate of the higher iodine oxides in the atmosphere is very uncertain, and within the *Base* scheme there is an increasing accumulation of I_xO_y with altitude. As a consequence, the percentage contribution of atomic iodine to I_y for the *Base* scheme is at least halved with respect to the $J_{I_xO_y}$ scheme. If I_xO_y species are not considered for the *Base* scheme, then the I/I_y contour lines for both simulations present equivalent values (see Sect. 3.4).

The tropical ring of atomic iodine is a photochemical phenomenon defined by the low abundance of ozone and cold conditions of the upper troposphere. While the absolute ambient levels of iodine species depend on the total inorganic loading of the tropical troposphere (i.e., washout rates, ice-uptake, etc.), the unusual feature of the halogen atom being the predominant species is an implicit consequence of the fast thermal/photochemical interplay within the main iodine chemistry cycling scheme (see Tables 1 and 2) and the natural state of the tropical upper troposphere (i.e., high photolysis rates, lower O₃ than in the stratosphere and low temperatures). As the I atom ring is photochemically driven, it is present only in the illuminated portion of the earth and it circles the tropics with the sun. Fernandez et al. (2014) have suggested a co-existent “tropical ring of atomic bromine” within the TTL. The driving mechanisms of these atomic halogen rings are identical, and the distinct features between their relative peak altitude or abundances are due to the different photodissociation rates for J_{IO} and J_{BrO} , and the different lifetimes of the organic VSL halocarbons that constitute the main source of reactive iodine (CH₃I) and bromine (mostly CHBr₃) in the upper tropical troposphere.

Iodine chemistry in the troposphere and its effect on ozone

A. Saiz-Lopez et al.

Title Page

Abstract

Introduction

Conclusions

References

Tables

Figures



Back

Close

Full Screen / Esc

Printer-friendly Version

Interactive Discussion



3.3.1 The I/IO ratio in the troposphere

As described above, atomic iodine levels surpass IO abundances above $\sim 5\text{--}6$ km, therefore a ratio $I/IO > 1$ must exist in the middle and upper troposphere. Figure 6a shows the vertical variation of the I/IO ratio for the *Base* and $J_{I_xO_y}$ schemes, averaged over different regions and periods within the tropics. A ratio of $I/IO > 1$ is calculated from the mid-troposphere through the tropical cold point tropopause. Notwithstanding the photochemical treatment of the higher iodine oxides, both schemes present identical I/IO vertical profiles with maximum values occurring at coincident altitudes ($\sim 14\text{--}15$ km or ~ 130 hPa), which indicate that the occurrence of $I/IO > 1$ is independent of I_y . The peak magnitude strongly depends on the local O_3 abundance and the cold temperatures prevailing in the upper troposphere (Fig. 6b). The ratio maximizes during periods, and within regions of strong convection, when poor-ozone air-masses are rapidly transported from the lower troposphere to the lower TTL, avoiding the intrusion of ozone-rich air-masses from the lower stratosphere. Then, both *Base* and $J_{I_xO_y}$ schemes show a ratio enhancement from $I/IO \approx 3$ for the tropical annual average to ~ 8 within the Western Pacific (WP) warm pool during February. Within the WP region and during a vigorous convective event transporting large amounts of inorganic iodine directly into the lower TTL, the model I/IO ratio reached values as high as ~ 20 for both schemes (Fig. 6a). This highlights the importance of measuring atomic iodine levels in the upper troposphere in order to constrain our current knowledge of the iodine burden in this region of the atmosphere.

The O_3 concentration and the ambient temperature are the dominant factors in determining the ratio. The ozone levels and surrounding temperatures determining the $I/IO > 1$ range from 25 ppbv to 200 ppbv and from 250 K to 190 K at the lower and higher boundary limit, respectively (Fig. 6b). Following a steady state approximation considering the two most important reactions involving I and IO species, the ratio can

Iodine chemistry in the troposphere and its effect on ozone

A. Saiz-Lopez et al.

Title Page

Abstract

Introduction

Conclusions

References

Tables

Figures



Back

Close

Full Screen / Esc

Printer-friendly Version

Interactive Discussion



be calculated using the IO photolysis and the I reaction with O₃:

$$\frac{[I]}{[IO]} = \frac{J_{IO}}{k_{I+O_3} [O_3]}. \quad (5)$$

Contribution from other species that react with atomic I is negligible (see Table 1).

Note that even when both schemes result in a similar ratio vertical profile, the $J_{I_xO_y}$ scheme calculates slightly smaller ratios because the assumed photochemical breakdown of I_xO_y releases IO radicals back to the gas phase, reducing the I/IO ratio.

The geographical distributions of the tropical ring of atomic iodine and the I/IO ratio at an altitude of 14 km are shown in Fig. 7. Results for the $J_{I_xO_y}$ scheme are presented since the maximum values of both the iodine ring and the ratio are coincident in altitude when the photolysis of I_xO_y are considered. Both distributions clearly maximize in the Western Pacific region and the Indian Ocean, highlighting the importance of convective transport and strength of oceanic sources in the occurrence of this natural phenomenon. The I/IO ratio follows the geographical distribution of O₃ and temperature, both of which locally minimize in the same region where the ratio peaks (Fig. 7c and d). Note also that I/IO > 1 only occurs within the tropical latitudes, decreasing to values smaller than unity polewards of 30° N/S. Hence, we suggest experimental programs oriented to reduce the uncertainties of iodine chemistry in the tropical troposphere should also include a strategy for the direct measurements of daytime atomic iodine besides the usually targeted IO radical.

3.4 The partitioning of inorganic iodine

Figure 8 shows the annual zonal average distribution of the main iodine species (besides atomic iodine) for the *Base* (left panels) and $J_{I_xO_y}$ (right panels) schemes. With the exception of IONO₂, which is the only species with a strong hemispheric gradient in the MBL due to the larger anthropogenic NO_x levels prevailing over the northern oceans, all inorganic iodine species abundances maximize within the tropical regions.

Title Page

Abstract

Introduction

Conclusions

References

Tables

Figures



Back

Close

Full Screen / Esc

Printer-friendly Version

Interactive Discussion



Iodine chemistry in the troposphere and its effect on ozone

A. Saiz-Lopez et al.

Title Page

Abstract

Introduction

Conclusions

References

Tables

Figures



Back

Close

Full Screen / Esc

Printer-friendly Version

Interactive Discussion



IO abundance in the FT is reduced to $\sim 1/3$ of its concentration in the MBL, maintaining an approximately constant abundance with height between 2 and 8 km. In the *Base* scheme, noon IO levels in the tropics ≥ 0.1 pptv between 2 and 7–8 km result from halogen recycling on sea-salt (active up to about 4–5 km) and photolysis of CH_3I . Above 7–8 km, and up to the tropopause, noon IO levels ≥ 0.1 pptv can only be sustained by the combined release of iodine atoms from the photodissociation of CH_3I , whose concentration is ~ 0.1 pptv from 4 to 12 km, and the photolysis of I_xO_y that increases the lifetime of IO_x in the gas phase (see Fig. 4).

Figure 8 shows that HOI is the dominant iodine species, representing more than 60 % of total I_y between 1 and 8 km for the $J_{\text{I}_x\text{O}_y}$ scheme (HOI is the dominant species both during the day and at night, see Figs. 3 and 11). HI and IONO_2 contributions represent less than 5 % of total I_y while IONO_2 exceeds 10 % in the lower troposphere of the Northern Hemisphere. Note how the abundance of I_xO_y increases significantly with altitude for the case of the *Base* scheme, due to decreasing temperatures that prevent their thermal decomposition (Fig. 8i). This shows that for the *Base* scheme there is a permanent conversion of the major active iodine species to I_xO_y , which turns out to be a non-reactive reservoir that does not recycle back to active IO_x (see gray shade in Fig. 9a). Up to 70 % of the total I_y is modeled to be transformed to unreactive I_xO_y in the upper troposphere within the *Base* scheme, representing a fundamental problem to our current knowledge of iodine chemistry. Even when the tropospheric washout efficiency of I_xO_y is assumed to be larger than that of HOI ($k_{\text{H}}^{\text{I}_x\text{O}_y} > k_{\text{H}}^{\text{HOI}}$, see Table 4), the higher oxides production is so large, and their thermal decomposition so slow, that their final fate within the *Base* scheme is to accumulate in the atmosphere. Either (i) an unrecognized removal processes for I_xO_y must exist in the FT and UT, or (ii) a decomposition pathway releasing active iodine, such as the photodecomposition proposed in the $J_{\text{I}_x\text{O}_y}$ scheme, occurs. As to the authors knowledge there are no evidence for (i), we then suggest, based on experimental and theoretical studies (i.e. Gómez Martín et al., 2005; Saiz-Lopez et al., 2008) that the photochemistry of I_xO_y should be further investigated in order to reduce uncertainties on the important chemical impacts of iodine

chemistry. With the assumptions made in the $J_{I_xO_y}$ scheme, the I_xO_y levels are clearly reduced in favor of other inorganic iodine species (see Fig. 9b), which strongly affect their potential impact on tropospheric ozone destruction (see Sect. 3.5).

Figure 9 shows the vertical variation of the contribution of organic and inorganic species to the total iodine burden within the tropical atmosphere. The only precursor species with a photochemical lifetime long enough to reach the UT is CH_3I , whose abundance remain at ~ 0.1 pptv until the lower TTL (~ 12 km) is reached. There is a small contribution of minor VSL iodocarbons (CH_2I_2 , CH_2IBr and CH_2ICl), but most of them are decomposed within the MBL. Note that below 5 km, there is also a non-negligible contribution of di-halogen molecules ($ICl + IBr + I_2$), which on average for the whole year, represent up to 0.25–0.30 pptv of I_y integrated within the tropical MBL. At the ocean surface, the modelled overall abundance of I_2 , ICl and IBr species at night time reaches 1.3 (1.7) pptv for the *Base* ($J_{I_xO_y}$) schemes, respectively (Fig. 3b). The predominant contribution of these diatomic species to nighttime I_y decreases rapidly with altitude due to the rapid reduction in the availability of sea-salt aerosol surface, upon which IBr and ICl are formed following the uptake and heterogeneous recycling of $IONO_2$, INO_2 and HOI (see Table 3). Additionally, an abiotic source of I_2 (as well as HOI) is introduced in the model at the ocean surface following the oxidative reaction of ozone with aqueous iodide (see Sect. 2.1). Within the tropics, approximately half of this inorganic oceanic flux is released during the night, resulting in the direct buildup of I_2 in the lower atmosphere, as well as an indirect buildup of ICl and IBr due to the heterogeneous recycling of HOI on sea-salt aerosols. Up to 50 % of the nighttime I_y within the MBL is in the form of $I_2 + IBr + ICl$. The relative contribution of I_2 , IBr and ICl to the overall di-halogen contributions within the MBL are, respectively, 68 %, 16 % and 16 % for the *Base* scheme, and 53 %, 23 % and 23 % for the $J_{I_xO_y}$ scheme. Note that the contribution of the minor iodine species (I_{minor}) represents less than 5 % of I_y in both schemes.

Compared to the organic portion, the inorganic fraction is the dominant component of the total iodine budget for both schemes, with I_y representing more than 90 % of total

Iodine chemistry in the troposphere and its effect on ozone

A. Saiz-Lopez et al.

Title Page

Abstract

Introduction

Conclusions

References

Tables

Figures



Back

Close

Full Screen / Esc

Printer-friendly Version

Interactive Discussion



iodine through the mid- to upper-troposphere (Fig. 9). This is in clear contrast to the bromine partitioning in the troposphere where even if the abundant long-lived Halons and CH_3Br are left aside and just VSL bromocarbons are considered, only 30–40 % of bromine is inorganic in the FT, with the dominant component being the organic VSL portion (Fernandez et al., 2014).

Figure 10 shows the annual additive zonal distribution of iodine species. Results are presented at selected heights of around 1, 3, 6, 9, 12 and 15 km for the *Base* (left panels) and the $J_{\text{I}_x\text{O}_y}$ (right panels) schemes. The rapid conversion of organic VSL iodocarbons (mainly CH_3I) to inorganic iodine as the altitude increases, and across latitudes, as well as the above mentioned accumulation of I_xO_y in the *Base* scheme, are clearly appreciated in Fig. 10. Note that even when the total inorganic loading for the $J_{\text{I}_x\text{O}_y}$ scheme is only 10–20 % larger than for the *Base* scheme, the absolute abundance of the main I_y species (HOI, I and IO) can be up to a factor of ~ 5 greater when I_xO_y are photolysed. Indeed, if I_xO_y are not considered when computing the total inorganic iodine for the *Base* scheme (i.e., defining an equivalent magnitude $\text{I}_y^* = \text{I}_y - \text{I}_x\text{O}_y$), then the relative contributions I/I_y^* , IO/I_y^* and HOI/I_y^* are equivalent to I/I_y , IO/I_y and HOI/I_y for the $J_{\text{I}_x\text{O}_y}$ scheme. This confirms the rapid establishment of the photochemical steady state for the gaseous iodine system and the inert role of I_xO_y on altering the I_y partitioning for the *Base* scheme, thereby indicating that I_xO_y production could basically be treated as an efficient sink of inorganic iodine, unless their photodissociation is considered.

For the same heights as Fig. 10, the average diurnal variation of the main iodine species is illustrated in Fig. 11. In the tropics, I and IO follow a diurnal concentration profile with a characteristic top-hat shape due to the fast photochemical constants of the iodine system which allows the rapid occurrence of the I-IO steady state. IO is the dominant daytime species below 5 km, while atomic iodine dominates above that height, defining the diurnal temporal evolution of the tropical I ring. IO levels show a double peak at twilight, which is most evident at lower altitudes. This is attributed to the reduced photodissociation of IO radical during sunrise and sunset, particularly at

Iodine chemistry in the troposphere and its effect on ozone

A. Saiz-Lopez et al.

[Title Page](#)[Abstract](#)[Introduction](#)[Conclusions](#)[References](#)[Tables](#)[Figures](#)[Back](#)[Close](#)[Full Screen / Esc](#)[Printer-friendly Version](#)[Interactive Discussion](#)

Iodine chemistry in the troposphere and its effect on ozone

A. Saiz-Lopez et al.

Title Page

Abstract

Introduction

Conclusions

References

Tables

Figures



Back

Close

Full Screen / Esc

Printer-friendly Version

Interactive Discussion



due to the reduced impact of anthropogenic O_3 precursors, as compared to the NH. The ($J_{I_xO_y} - Base$) differences shown in Fig. 12b are of the same magnitude as those found between a pair of simulations including (*OnlyBr*) and neglecting the bromine contributions from VSL bromocarbons (*NoVSL*). This suggests that the uncertainties on the impact of iodine chemistry on the ozone budget (i.e. uncertainties in the photochemistry of I_xO_y) are of the same magnitude as the overall impact of tropospheric bromine chemistry from VSLs (*OnlyBr- NoVSL*, Fig. 12d). Indeed, even when the lower atmospheric iodine loading is considered (*Base - OnlyBr*, Fig. 12c) the impact on tropospheric ozone at ~ 5 km (400–500 hPa) is at least twice that of the simulation with only bromine chemistry, mostly in the free and upper troposphere. This all highlights the need for further experimental research on the photochemical characterization of I_xO_y .

Figure 13 presents the absolute (Fig. 13a) and relative (Fig. 13b) vertical range of ozone loss rate between the *Base* and $J_{I_xO_y}$ schemes for each chemical family that participates in tropospheric odd oxygen (O_x) loss cycles. The formalism of O_x loss rates computations is presented in Table 5 based on the catalytic cycles and families defined in Brasseur and Solomon (2006), with the inclusion of iodine-driven O_x chemical losses ($IO_{x_{Loss}}$). The direct O_x loss rate ($O_{x_{Loss}}$) represents the major ozone depleting family within the tropical MBL and FT, while in the upper troposphere the $HO_{x_{Loss}}$ cycles become the predominant loss processes up to the tropical tropopause. Within the MBL, and as a consequence of the increased inorganic iodine loading due to the direct oceanic injection of reactive I_2/HOI species, $IO_{x_{Loss}}$ cycles represent the second most important ozone depleting family ($IO_{x_{Loss}}^{MBL} \approx 17\%$ (27%) for *Base* ($J_{I_xO_y}$), respectively), surpassing in efficiency the contribution of $HO_{x_{Loss}}$. Comparatively, the overall effect of $BrO_x + ClO_x$ cycles constitute an ozone loss contribution smaller than 3% in the MBL, reaching a percentage contribution $> 10\%$ only in the upper-troposphere. Note that our modelled daytime BrO levels averaged within the tropical MBL are $\sim(0.2-0.3)$ pptv, with higher values of up to a few pptv calculated within coastal locations and regions of strong convection (Fernandez et al., 2014). Notably, the iodine impact on the

Iodine chemistry in the troposphere and its effect on ozone

A. Saiz-Lopez et al.

Title Page

Abstract

Introduction

Conclusions

References

Tables

Figures



Back

Close

Full Screen / Esc

Printer-friendly Version

Interactive Discussion



acceleration of ozone loss cycles peaks in the UT (that is, within the extensive tropical ring of atomic iodine), with a maximum contribution to the total ozone loss of 0.06 (0.1) ppbv day⁻¹ (representing 14 (35) % of total loss) reached at 11 (13) km of altitude, for the *Base* ($J_{I_xO_y}$) schemes, respectively. Our results indicate that, on average for the whole troposphere, iodine mediated ozone losses are responsible for at least 70–85 % of the total ozone depletion due to halogens.

The differences between $IO_{x_{Loss}}$ and $BrO_x - ClO_{x_{Loss}}$ contributions can be explained based on the higher reactivity and therefore shorter lifetimes of iodine species: (i) due to the comparatively longer lifetimes of organic bromo- and chloro-carbons, inorganic bromine and chlorine cycles represent a major ozone loss process in the lower and middle stratosphere (Salawitch et al., 2005); and (ii) the very fast catalytic reactions of iodine species make IO_x ozone loss cycles to be up to 10 times faster than $BrO_x - ClO_x$ cycles for an identical I_y and Br_y basis (i.e. $IO_{x_{Loss}}/I_y \approx 10 \times ClO_x - BrO_{x_{Loss}}/Br_y$). The total I_y abundance at the height where the relative $IO_{x_{Loss}}$ maximizes (~ 12 km) is in the range (0.66–0.81) pptv for the (*Base*– $J_{I_xO_y}$) schemes, while for bromine, $Br_y^{12km} \approx 1.0$ pptv and $Br_y^{17km} \approx 3.0$ pptv (Fernandez et al., 2014), indicating that even when Br_y abundances are larger in the upper troposphere, the greater O_3 destruction efficiency of IO_x makes iodine the dominant halogen contributing to tropospheric ozone loss, throughout the tropics and mid-latitudes (see Table 6). Indeed, our results show that iodine-driven ozone loss cycles are the second most important ozone depleting family both in the tropical MBL and in the tropical and mid-latitude upper troposphere. Therefore we suggest global models oriented to estimate past and future projections of tropospheric ozone burden and trends should include at least a simplified description of tropospheric iodine sources and inorganic chemistry, in addition to bromine.

Table 6 summarises the integrated ozone column and the averaged ozone loss rate for different altitude intervals within the troposphere (MBL, FT, UT and total troposphere) within the tropical and mid-latitude regions. With the $J_{I_xO_y}$ scheme, the total tropospheric O_3 column is ~ 1 DU smaller than for the *Base* scheme, representing

Iodine chemistry in the troposphere and its effect on ozone

A. Saiz-Lopez et al.

Title Page

Abstract

Introduction

Conclusions

References

Tables

Figures



Back

Close

Full Screen / Esc

Printer-friendly Version

Interactive Discussion



an additional 4–7% reduction of tropospheric ozone. Adding up the contribution of bromine and iodine from VSL sources, and gas and heterogeneous chemistry, the tropical tropospheric O₃ column for the $J_{I_xO_y}$ scheme is reduced by 2.6 DU relative to the *NoVSL* simulation, representing more than 10% of the total tropospheric column.

As reported previously (Saiz-Lopez et al., 2012b) approx. 80% of the ozone loss in the tropical troposphere occurs within the FT and UT, representing the FT approximately half of the total tropospheric column losses.

Table 6 also presents the relative contribution of each of the odd oxygen families averaged at different altitude intervals and latitudinal bands. The overall impact of iodine chemistry on tropospheric ozone is larger in the tropics than within the mid-latitudes, due to greater I/IO ratio and larger contribution of IO_x to total inorganic iodine within the I atom tropical ring. Even when the change in the tropospheric ozone column between the $J_{I_xO_y}$ and *Base* schemes is of similar magnitude for the tropics and the mid-latitudes ($\Delta_{O_3}^{Tropics} \approx -1.0$ DU and $\Delta_{O_3}^{Midlats} \approx -1.1$ DU), the ozone loss acceleration due to the increase in iodine loading is ~ 2 times larger for the $J_{I_xO_y}$ scheme within the tropics ($\Delta_{O_3Loss}^{Tropics} \approx 26.2$ DU yr⁻¹ and $\Delta_{O_3Loss}^{Midlats} \approx 11.7$ DU yr⁻¹). Our results indicate that the integrated contribution of the iodine system to the total rate of tropospheric ozone loss over the tropics is 2.2 (5.3) times larger than that of chlorine and bromine chemistry for the *Base* ($J_{I_xO_y}$) schemes, compared to a 1.2 (2.4) relative enhancement over the mid-latitudes. Notably, in the MBL iodine-mediated ozone loss rate is almost an order of magnitude faster than the combined rates of BrO_x + ClO_x cycles, even when the *Base* scheme is considered. Within the lower TTL, BrO_x–ClO_{xLoss} catalytic cycles result in higher ozone losses than IO_{xLoss} cycles only for the *Base* simulation. Note however that if photolysis of higher iodine oxides is allowed in the model, the IO_x catalytic ozone depleting cycles continue to be more efficient than BrO_x–ClO_{xLoss} cycles throughout most of the TTL (Fig. 13).

4 Summary and conclusions

We propose the existence of a “tropical ring of atomic iodine” that circles the tropics with the sun. The tropical ring extends from 30° S to 30° N and maximizes at a height of 11–14 km, with vmr ranging from 0.2 to 0.8 pptv. This photochemical phenomenon is driven by the fast photolysis rate of IO and the Arrhenius behaviour of the I + O₃ reaction, and appears naturally in the upper troposphere where ambient temperature minimize and ozone abundances are at least one order of magnitude below stratospheric levels. Within this tropical ring, annual average I/IO ratios of ~ 3 are modelled, reaching maximum values of ~ 20 during events of vigorous convection. Inorganic iodine surpasses the contribution of organic VSL species throughout the troposphere, being CH₃I the dominant source that maintains I_y levels in the FT and UT. Within the MBL and FT, HOI is the dominant I_y species, both during the day and at night. The other abundant night-time reservoirs are IONO₂ in the UT and the di-halogen molecules (I₂, IBr and ICl) in the MBL.

Finally, we suggest that reducing uncertainties on the photochemistry of I_xO_y species constitutes the main challenge to our current knowledge of atmospheric iodine chemistry. We show that if the photodissociation of I_xO_y is neglected, then these higher oxides accumulate in the atmosphere due to their slow thermal decomposition and became an effective sink of active iodine in the FT and UT. Experimental and theoretical studies on the I_xO_y photochemistry are required to improve the knowledge on the inorganic iodine burden and its oxidative impacts in the troposphere. Based on our modelled range of inorganic iodine loading (0.7–1.0) pptv in the FT dependent on the consideration or not of I_xO_y photolysis, we show for the first time with a global model that iodine is the second most important ozone-depleting family in the tropical MBL and in the global marine UT, representing between (17–27) % and (11–27) % of the total ozone loss. Therefore, we suggest global chemistry-climate models (CCMs) should include at least a simplified representation of iodine tropospheric chemistry for

Iodine chemistry in the troposphere and its effect on ozone

A. Saiz-Lopez et al.

[Title Page](#)[Abstract](#)[Introduction](#)[Conclusions](#)[References](#)[Tables](#)[Figures](#)[Back](#)[Close](#)[Full Screen / Esc](#)[Printer-friendly Version](#)[Interactive Discussion](#)

future CCM-Validation and CCM-Intercomparison projects concerned with tropospheric ozone over the oceans for past, present and future scenarios.

Acknowledgements. This work was supported by the Consejo Superior de Investigaciones Cientificas (CSIC), Spain. The National Center for Atmospheric Research (NCAR) is funded by the National Science Foundation NSF. Computing resources (ark:/85065/d7wd3xhc) were provided by the Climate Simulation Laboratory at NCAR's Computational and Information Systems Laboratory (CISL), sponsored by the NSF and other agencies. The CESM project (which includes CAM-Chem) is supported by the NSF and the Office of Science (BER) of the US Department of Energy. This work was also sponsored by the NASA Atmospheric Composition Modeling and Analysis Program Activities (ACMAP), grant/cooperative agreement number NNX11AH90G. The authors are grateful to J. M. C. Plane for support and helpful discussions. R. P. F. would like to thank ANPCyT (PICT-PRH 2009-0063) and SeCTyP-UNCuyo for financial support.

References

- Alicke, B., Hebestreit, K., Stutz, J., and Platt, U.: Iodine oxide in the marine boundary layer, *Nature*, 397, 572–573, doi:10.1038/17508, 1999.
- Allan, B. J. and Plane, J. M. C.: A study of the recombination of IO with NO₂ and the stability of INO₃?: Implications for the atmospheric chemistry of iodine, *J. Phys. Chem. A*, 106, 8634–8641, doi:10.1021/jp020089q, 2002.
- Allan, B. J., McFiggans, G., Plane, J. M. C., and Coe, H.: Observations of iodine monoxide in the remote marine boundary layer, *J. Geophys. Res.*, 105, 14363, doi:10.1029/1999JD901188, 2000.
- Atkinson, H. M., Huang, R.-J., Chance, R., Roscoe, H. K., Hughes, C., Davison, B., Schönhardt, A., Mahajan, A. S., Saiz-Lopez, A., Hoffmann, T., and Liss, P. S.: Iodine emissions from the sea ice of the Weddell Sea, *Atmos. Chem. Phys.*, 12, 11229–11244, doi:10.5194/acp-12-11229-2012, 2012.
- Atkinson, R., Baulch, D. L., Cox, R. A., Crowley, J. N., Hampson, R. F., Hynes, R. G., Jenkin, M. E., Rossi, M. J., and Troe, J.: Evaluated kinetic and photochemical data for atmospheric chemistry: Volume III – gas phase reactions of inorganic halogens, *Atmos. Chem. Phys.*, 7, 981–1191, doi:10.5194/acp-7-981-2007, 2007.

20012

ACPD

14, 19985–20044, 2014

Iodine chemistry in the troposphere and its effect on ozone

A. Saiz-Lopez et al.

Title Page

Abstract

Introduction

Conclusions

References

Tables

Figures



Back

Close

Full Screen / Esc

Printer-friendly Version

Interactive Discussion



Iodine chemistry in the troposphere and its effect on ozone

A. Saiz-Lopez et al.

[Title Page](#)[Abstract](#)[Introduction](#)[Conclusions](#)[References](#)[Tables](#)[Figures](#)[Back](#)[Close](#)[Full Screen / Esc](#)[Printer-friendly Version](#)[Interactive Discussion](#)

Atkinson, R., Baulch, D. L., Cox, R. A., Crowley, J. N., Hampson, R. F., Hynes, R. G., Jenkin, M. E., Rossi, M. J., Troe, J., and Wallington, T. J.: Evaluated kinetic and photochemical data for atmospheric chemistry: Volume IV – gas phase reactions of organic halogen species, *Atmos. Chem. Phys.*, 8, 4141–4496, doi:10.5194/acp-8-4141-2008, 2008.

5 Bale, C. S. E., Ingham, T., Commane, R., Heard, D. E., and Bloss, W. J.: Novel measurements of atmospheric iodine species by resonance fluorescence, *J. Atmos. Chem.*, 60, 51–70, doi:10.1007/s10874-008-9108-z, 2008.

Bedjanian, Y., Le Bras, G., and Poulet, G.: Kinetic study of the Br + IO, I + BrO and Br + I₂ reactions, heat of formation of the BrO radical, *Chem. Phys. Lett.*, 266, 233–238, doi:10.1016/S0009-2614(97)01530-3, 1997.

10 Bell, N., Hsu, L., Jacob, D. J., Schultz, M. G., Blake, D. R., Butler, J. H., King, D. B., Lobert, J. M., and Maier-Reimer, E.: Methyl iodide: atmospheric budget and use as a tracer of marine convection in global models, *J. Geophys. Res.*, 107, 4340, doi:10.1029/2001JD001151, 2002.

Bloss, W. J., Rowley, D. M., Cox, R. A., and Jones, R. L.: Kinetics and products of the IO self-reaction, *J. Phys. Chem. A*, 105, 7840–7854, doi:10.1021/jp0044936, 2001.

15 Bloss, W. J., Lee, J. D., Johnson, G. P., Sommariva, R., Heard, D. E., Saiz-Lopez, A., Plane, J. M., McFiggans, G. B., Coe, H., Flynn, M., Williams, P., Rickard, A. R., and Fleming, Z. L.: Impact of halogen monoxide chemistry upon boundary layer OH and HO₂ concentrations at a coastal site, *Geophys. Res. Lett.*, 32, L06814, doi:10.1029/2004GL022084, 2005.

20 Bösch, H., Camy-Peyret, C., Chipperfield, M. P., Fitzenberger, R., Harder, H., Platt, U., and Pfeilsticker, K.: Upper limits of stratospheric IO and OIO inferred from center-to-limb-darkening-corrected balloon-borne solar occultation visible spectra: implications for total gaseous iodine and stratospheric ozone, *J. Geophys. Res.*, 108, 4455, doi:10.1029/2002JD003078, 2003.

25 Brasseur, G. and Solomon, S.: *Aeronomy of the Middle Atmosphere: chemistry and Physics of the Stratosphere and Mesosphere*, 3rd edition, Springer, Dordrecht, the Netherlands, 2005.

Butz, A., Bösch, H., Camy-Peyret, C., Chipperfield, M. P., Dorf, M., Kreycky, S., Kritten, L., Prados-Román, C., Schwärzle, J., and Pfeilsticker, K.: Constraints on inorganic gaseous iodine in the tropical upper troposphere and stratosphere inferred from balloon-borne solar occultation observations, *Atmos. Chem. Phys.*, 9, 7229–7242, doi:10.5194/acp-9-7229-2009, 2009.

5
10
15
20
25
30

Iodine chemistry in the troposphere and its effect on ozone

A. Saiz-Lopez et al.

Title Page

Abstract

Introduction

Conclusions

References

Tables

Figures



Back

Close

Full Screen / Esc

Printer-friendly Version

Interactive Discussion



Calvert, J. G. and Lindberg, S. E.: Potential influence of iodine-containing compounds on the chemistry of the troposphere in the polar spring, I. Ozone depletion, *Atmos. Environ.*, **38**, 5087–5104, doi:10.1016/j.atmosenv.2004.05.049, 2004.

Carpenter, L. J., Archer, S. D., and Beale, R.: Ocean–atmosphere trace gas exchange, *Chem. Soc. Rev.*, **41**, 6473–506, doi:10.1039/c2cs35121h, 2012.

Carpenter, L. J., MacDonald, S. M., Shaw, M. D., Kumar, R., Saunders, R. W., Parthipan, R., Wilson, J., and Plane, J. M. C.: Atmospheric iodine levels influenced by sea surface emissions of inorganic iodine, *Nat. Geosci.*, **6**, 108–111, doi:10.1038/ngeo1687, 2013.

Chambers, R. M., Heard, A. C., and Wayne, R. P.: Inorganic gas-phase reactions of the nitrate radical: iodine + nitrate radical and iodine atom + nitrate radical, *J. Phys. Chem.*, **96**, 3321–3331, doi:10.1021/j100187a028, 1992.

Chameides, W. L. and Davis, D. D.: Iodine: its possible role in tropospheric photochemistry, *J. Geophys. Res.*, **85**, 7383, doi:10.1029/JC085iC12p07383, 1980.

Daehlie, G. and Kjekshus, A.: Iodine Oxides, *Acta Chem. Scand.*, **18**, 114–156, 1964.

Dillon, T. J., Karunanandan, R., and Crowley, J. N.: The reaction of IO with CH₃SCH₃: products and temperature dependent rate coefficients by laser induced fluorescence, *Phys. Chem. Chem. Phys.*, **8**, 847–55, doi:10.1039/b514718b, 2006.

Dillon, T. J., Tucceri, M. E., Sander, R., and Crowley, J. N.: LIF studies of iodine oxide chemistry, Part 3. Reactions IO + NO₃ → OIO + NO₂, I + NO₃ → IO + NO₂, and CH₂I + O₂ → (products): implications for the chemistry of the marine atmosphere at night, *Phys. Chem. Chem. Phys.*, **10**, 1540–54, doi:10.1039/b717386e, 2008.

Dix, B., Baidar, S., Bresch, J. F., Hall, S. R., Schmidt, K. S., Wang, S., and Volkamer, R.: Detection of iodine monoxide in the tropical free troposphere., *P. Natl. Acad. Sci. USA*, **110**, 2035–40, doi:10.1073/pnas.1212386110, 2013.

Emmons, L. K., Walters, S., Hess, P. G., Lamarque, J.-F., Pfister, G. G., Fillmore, D., Granier, C., Guenther, A., Kinnison, D., Laepple, T., Orlando, J., Tie, X., Tyndall, G., Wiedinmyer, C., Baughcum, S. L., and Kloster, S.: Description and evaluation of the Model for Ozone and Related chemical Tracers, version 4 (MOZART-4), *Geosci. Model Dev.*, **3**, 43–67, doi:10.5194/gmd-3-43-2010, 2010.

Fernandez, R. P., Salawitch, R. J., Kinnison, D. E., Lamarque, J.-F., and Saiz-Lopez, A.: Bromine partitioning in the tropical tropopause layer: implications for stratospheric injection, *Atmos. Chem. Phys. Discuss.*, **14**, 17857–17905, doi:10.5194/acpd-14-17857-2014, 2014.

Iodine chemistry in the troposphere and its effect on ozone

A. Saiz-Lopez et al.

[Title Page](#)[Abstract](#)[Introduction](#)[Conclusions](#)[References](#)[Tables](#)[Figures](#)[Back](#)[Close](#)[Full Screen / Esc](#)[Printer-friendly Version](#)[Interactive Discussion](#)

Gálvez, O., Gómez Martín, J. C., Gómez, P. C., Saiz-Lopez, A., and Pacios, L. F.: A theoretical study on the formation of iodine oxide aggregates and monohydrates, *Phys. Chem. Chem. Phys.*, 15, 15572–83, doi:10.1039/c3cp51219c, 2013.

Garland, J. A. and Curtis, H.: Emission of iodine from the sea surface in the presence of ozone, *J. Geophys. Res.*, 86, 3183, doi:10.1029/JC086iC04p03183, 1981.

Gilles, M. K., Turnipseed, A. A., Burkholder, J. B., and Ravishankara, A. R.: A study of the $\text{Br} + \text{IO} \rightarrow \text{I} + \text{BrO}$ and the reverse reaction, *Chem. Phys. Lett.*, 272, 75–82, doi:10.1016/S0009-2614(97)00485-5, 1997.

Glowacki, D. R., Liang, C.-H., Morley, C., Pilling, M. J., and Robertson, S. H.: MESMER: an open-source master equation solver for multi-energy well reactions, *J. Phys. Chem. A*, 116, 9545–60, doi:10.1021/jp3051033, 2012.

Gómez Martín, J. C. and Plane, J. M. C.: Determination of the O–IO bond dissociation energy by photofragment excitation spectroscopy, *Chem. Phys. Lett.*, 474, 79–83, 2009.

Gómez Martín, J. C., Spietz, P., and Burrows, J. P.: Spectroscopic studies of the I_2/O_3 photochemistry, Part 1: Determination of the absolute absorption cross sections of iodine oxides of atmospheric relevance, *J. Photoch. Photobio. A*, 176, 15–38, doi:10.1016/j.jphotochem.2005.09.024, 2005.

Gómez Martín, J. C., Spietz, P., and Burrows, J. P.: Kinetic and mechanistic studies of the $\text{I}(2)/\text{O}(3)$ photochemistry, *J. Phys. Chem. A*, 111, 306–20, doi:10.1021/jp061186c, 2007.

Gómez Martín, J. C., Gálvez, O., Baeza-Romero, M. T., Ingham, T., Plane, J. M. C., and Blitz, M. A.: On the mechanism of iodine oxide particle formation, *Phys. Chem. Chem. Phys.*, 15, 15612–22, doi:10.1039/c3cp51217g, 2013a.

Gómez Martín, J. C., Mahajan, A. S., Hay, T. D., Prados-Román, C., Ordóñez, C., MacDonald, S. M., Plane, J. M. C., Sorribas, M., Gil, M., Paredes Mora, J. F., Agama Reyes, M. V., Oram, D. E., Leedham, E., and Saiz-Lopez, A.: Iodine chemistry in the eastern Pacific marine boundary layer, *J. Geophys. Res.-Atmos.*, 118, 887–904, doi:10.1002/jgrd.50132, 2013b.

Großmann, K., Frieß, U., Peters, E., Wittrock, F., Lampel, J., Yilmaz, S., Tschirner, J., Sommariva, R., von Glasow, R., Quack, B., Krüger, K., Pfeilsticker, K., and Platt, U.: Iodine monoxide in the Western Pacific marine boundary layer, *Atmos. Chem. Phys.*, 13, 3363–3378, doi:10.5194/acp-13-3363-2013, 2013.

Hayase, S., Yabushita, A., Kawasaki, M., Enami, S., Hoffmann, M. R., and Colussi, A. J.: Heterogeneous reaction of gaseous ozone with aqueous iodide in the presence of aqueous organic species, *J. Phys. Chem. A*, 114, 6016–21, doi:10.1021/jp101985f, 2010.

Iodine chemistry in the troposphere and its effect on ozone

A. Saiz-Lopez et al.

Title Page

Abstract

Introduction

Conclusions

References

Tables

Figures



Back

Close

Full Screen / Esc

Printer-friendly Version

Interactive Discussion



- Hoffmann, T., O'Dowd, C., and Seinfeld, J.: Iodine oxide homogeneous nucleation: an explanation for coastal new particle production, *Geophys. Res. Lett.*, 28, 1949–1952, 2001.
- Huang, R. J., Seitz, K., Neary, T., O'Dowd, C. D., Platt, U., and Hoffmann, T.: Observations of high concentrations of I_2 and IO in coastal air supporting iodine-oxide driven coastal new particle formation, *Geophys. Res. Lett.*, 37, L03803, doi:10.1029/2009GL041467, 2010.
- Jenkin, M. E., Cox, R. A., and Candeland, D. E.: Photochemical aspects of tropospheric iodine behaviour, *J. Atmos. Chem.*, 2, 359–375, doi:10.1007/BF00130748, 1985.
- Jimenez, J. L., Bahreini, R., Cocker III, R., Zhuang, H., Varutbanhkul, V., Flagan, R., Seinfeld, J., O'Dowd, C., and Hoffmann, T.: New particle formation from photooxidation of diiodomethane (CH_2I_2), *J. Geophys. Res.*, 108, 4318, doi:10.1029/2002JD002452, 2003.
- Jones, C. E., Hornsby, K. E., Sommariva, R., Dunk, R. M., von Glasow, R., McFiggans, G., and Carpenter, L. J.: Quantifying the contribution of marine organic gases to atmospheric iodine, *Geophys. Res. Lett.*, 37, L18804, doi:10.1029/2010GL043990, 2010.
- Kaltsoyannis, N. and Plane, J. M. C.: Quantum chemical calculations on a selection of iodine-containing species (IO, OIO, INO_3 , $(IO)_2$, I_2O_3 , I_2O_4 and I_2O_5) of importance in the atmosphere., *Phys. Chem. Chem. Phys.*, 10, 1723–33, doi:10.1039/b715687c, 2008.
- Kinnison, D. E., Brasseur, G. P., Walters, S., Garcia, R. R., Marsh, D. R., Sassi, F., Harvey, V. L., Randall, C. E., Emmons, L., Lamarque, J. F., Hess, P., Orlando, J. J., Tie, X. X., Randel, W., Pan, L. L., Gettelman, A., Granier, C., Diehl, T., Niemeier, U., and Simmons, A. J.: Sensitivity of chemical tracers to meteorological parameters in the MOZART-3 chemical transport model, *J. Geophys. Res.*, 112, D20302, doi:10.1029/2006JD007879, 2007.
- Lamarque, J.-F., Emmons, L. K., Hess, P. G., Kinnison, D. E., Tilmes, S., Vitt, F., Heald, C. L., Holland, E. A., Lauritzen, P. H., Neu, J., Orlando, J. J., Rasch, P. J., and Tyndall, G. K.: CAM-chem: description and evaluation of interactive atmospheric chemistry in the Community Earth System Model, *Geosci. Model Dev.*, 5, 369–411, doi:10.5194/gmd-5-369-2012, 2012.
- Lancar, I. T., Mellouki, A., and Poulet, G.: Kinetics of the reactions of hydrogen iodide with hydroxyl and nitrate radicals, *Chem. Phys. Lett.*, 177, 554–558, doi:10.1016/0009-2614(91)90083-L, 1991.
- Laszlo, B., Huie, R. E., Kurylo, M. J., and Miziolek, A. W.: Kinetic studies of the reactions of BrO and IO radicals, *J. Geophys. Res.*, 102, 1523, doi:10.1029/96JD00458, 1997.
- Lawler, M. J., Mahajan, A. S., Saiz-Lopez, A., and Saltzman, E. S.: Observations of I_2 at a remote marine site, *Atmos. Chem. Phys.*, 14, 2669–2678, doi:10.5194/acp-14-2669-2014, 2014.

Iodine chemistry in the troposphere and its effect on ozone

A. Saiz-Lopez et al.

[Title Page](#)[Abstract](#)[Introduction](#)[Conclusions](#)[References](#)[Tables](#)[Figures](#)[Back](#)[Close](#)[Full Screen / Esc](#)[Printer-friendly Version](#)[Interactive Discussion](#)

- MacDonald, S. M., Gómez Martín, J. C., Chance, R., Warriner, S., Saiz-Lopez, A., Carpenter, L. J., and Plane, J. M. C.: A laboratory characterisation of inorganic iodine emissions from the sea surface: dependence on oceanic variables and parameterisation for global modelling, *Atmos. Chem. Phys.*, 14, 5841–5852, doi:10.5194/acp-14-5841-2014, 2014.
- 5 Mahajan, A. S., Plane, J. M. C., Oetjen, H., Mendes, L., Saunders, R. W., Saiz-Lopez, A., Jones, C. E., Carpenter, L. J., and McFiggans, G. B.: Measurement and modelling of tropospheric reactive halogen species over the tropical Atlantic Ocean, *Atmos. Chem. Phys.*, 10, 4611–4624, doi:10.5194/acp-10-4611-2010, 2010.
- 10 Mahajan, A. S., Sorribas, M., Gómez Martín, J. C., MacDonald, S. M., Gil, M., Plane, J. M. C., and Saiz-Lopez, A.: Concurrent observations of atomic iodine, molecular iodine and ultrafine particles in a coastal environment, *Atmos. Chem. Phys.*, 11, 2545–2555, doi:10.5194/acp-11-2545-2011, 2011.
- 15 Mahajan, A. S., Gómez Martín, J. C., Hay, T. D., Royer, S.-J., Yvon-Lewis, S., Liu, Y., Hu, L., Prados-Roman, C., Ordóñez, C., Plane, J. M. C., and Saiz-Lopez, A.: Latitudinal distribution of reactive iodine in the Eastern Pacific and its link to open ocean sources, *Atmos. Chem. Phys.*, 12, 11609–11617, doi:10.5194/acp-12-11609-2012, 2012.
- McFiggans, G., Plane, J. M. C., Allan, B. J., Carpenter, L. J., Coe, H., and O'Dowd, C.: A modelling study of iodine chemistry in the marine boundary layer, *J. Geophys. Res.*, 105, 14371–14385, doi:10.1029/1999JD901187, 2000.
- 20 McFiggans, G., Coe, H., Burgess, R., Allan, J., Cubison, M., Alfarra, M. R., Saunders, R., Saiz-Lopez, A., Plane, J. M. C., Wevill, D., Carpenter, L., Rickard, A. R., and Monks, P. S.: Direct evidence for coastal iodine particles from *Laminaria* macroalgae – linkage to emissions of molecular iodine, *Atmos. Chem. Phys.*, 4, 701–713, doi:10.5194/acp-4-701-2004, 2004.
- 25 McFiggans, G., Bale, C. S. E., Ball, S. M., Beames, J. M., Bloss, W. J., Carpenter, L. J., Dorsey, J., Dunk, R., Flynn, M. J., Furneaux, K. L., Gallagher, M. W., Heard, D. E., Hollingsworth, A. M., Hornsby, K., Ingham, T., Jones, C. E., Jones, R. L., Kramer, L. J., Langridge, J. M., Leblanc, C., LeCrane, J.-P., Lee, J. D., Leigh, R. J., Longley, I., Mahajan, A. S., Monks, P. S., Oetjen, H., Orr-Ewing, A. J., Plane, J. M. C., Potin, P., Shillings, A. J. L., Thomas, F., von Glasow, R., Wada, R., Whalley, L. K., and Whitehead, J. D.: Iodine-mediated coastal particle formation: an overview of the Reactive Halogens in the Marine Boundary Layer (RHAMBLE) Roscoff coastal study, *Atmos. Chem. Phys.*, 10, 2975–2999, doi:10.5194/acp-10-2975-2010, 2010.
- 30

Iodine chemistry in the troposphere and its effect on ozone

A. Saiz-Lopez et al.

Title Page

Abstract

Introduction

Conclusions

References

Tables

Figures



Back

Close

Full Screen / Esc

Printer-friendly Version

Interactive Discussion



Montzka, S. a., Reimann, S., Engel, A., Krüger, K., O'Doherty, S., and Sturges, W. T.: Ozone-depleting substances (odss) and related chemicals, in: Scientific Assessment of Ozone Depletion: 2010, Global Ozone Research and Monitoring Project-Report No. 52, Geneva, Switzerland, 1.1–1.108, 2011.

5 Mössinger, J. C., Shallcross, D. E., and Anthony Cox, R.: UV–VIS absorption cross-sections and atmospheric lifetimes of CH_2Br_2 , CH_2I_2 and CH_2BrI , *J. Chem. Soc. Faraday T.*, 94, 1391–1396, doi:10.1039/a709160e, 1998.

Neu, J. L. and Prather, M. J.: Toward a more physical representation of precipitation scavenging in global chemistry models: cloud overlap and ice physics and their impact on tropospheric ozone, *Atmos. Chem. Phys.*, 12, 3289–3310, doi:10.5194/acp-12-3289-2012, 2012.

10 O'Dowd, C., Jimenez, J., Bahreini, R., Flagan, R., Seinfeld, J., Hameri, K., Pirjola, L., Kulmala, M., Jennings, S. G., and Hoffmann, T.: Marine aerosol formation from biogenic iodine emissions, *Nature*, 417, 1–5, doi:10.1038/nature00775, 2002.

Ordóñez, C., Lamarque, J.-F., Tilmes, S., Kinnison, D. E., Atlas, E. L., Blake, D. R., Sousa Santos, G., Brasseur, G., and Saiz-Lopez, A.: Bromine and iodine chemistry in a global chemistry-climate model: description and evaluation of very short-lived oceanic sources, *Atmos. Chem. Phys.*, 12, 1423–1447, doi:10.5194/acp-12-1423-2012, 2012.

15 Parrish, D. D., Lamarque, J.-F., Naik, V., Horowitz, L., Shindell, D. T., Staehelin, J., Derwent, R., Cooper, O. R., Tanimoto, H., Volz-Thomas, A., Gilge, S., Scheel, H.-E., Steinbacher, M., and Fröhlich, M.: Long-term changes in lower tropospheric baseline ozone concentrations: comparing chemistry-climate models and observations at northern midlatitudes, *J. Geophys. Res.-Atmos.*, 119, 5719–5736, doi:10.1002/2013JD021435, 2014.

Pechtl, S., Lovejoy, E. R., Burkholder, J. B., and von Glasow, R.: Modeling the possible role of iodine oxides in atmospheric new particle formation, *Atmos. Chem. Phys.*, 6, 505–523, doi:10.5194/acp-6-505-2006, 2006.

25 Plane, J. M. C., Joseph, D. M., Allan, B. J., Ashworth, S. H., and Francisco, J. S.: An experimental and theoretical study of the reactions $\text{OIO} + \text{NO}$ and $\text{OIO} + \text{OH}$, *J. Phys. Chem. A*, 110, 93–100, doi:10.1021/jp055364y, 2006.

Puentedura, O., Gil, M., Saiz-Lopez, A., Hay, T., Navarro-Comas, M., Gómez-Pelaez, A., Cuevas, E., Iglesias, J., and Gomez, L.: Iodine monoxide in the north subtropical free troposphere, *Atmos. Chem. Phys.*, 12, 4909–4921, doi:10.5194/acp-12-4909-2012, 2012.

5
10
15
20
25
30

Iodine chemistry in the troposphere and its effect on ozone

A. Saiz-Lopez et al.

Title Page

Abstract

Introduction

Conclusions

References

Tables

Figures



Back

Close

Full Screen / Esc

Printer-friendly Version

Interactive Discussion



Rattigan, O. V., Shallcross, D. E., and Anthony Cox, R.: UV absorption cross-sections and atmospheric photolysis rates of CF_3I , CH_3I , $\text{C}_2\text{H}_5\text{I}$ and CH_2ICl , *J. Chem. Soc. Faraday T.*, 93, 2839–2846, doi:10.1039/a701529a, 1997.

Rayner, N. A.: Global analyses of sea surface temperature, sea ice, and night marine air temperature since the late nineteenth century, *J. Geophys. Res.*, 108, 4407, doi:10.1029/2002JD002670, 2003.

Roehl, C. M., Burkholder, J. B., Moortgat, G. K., Ravishankara, A. R., and Crutzen, P. J.: Temperature dependence of UV absorption cross sections and atmospheric implications of several alkyl iodides, *J. Geophys. Res.*, 102, 12819–12829, doi:10.1029/97JD00530, 1997.

Saiz-Lopez, A. and Plane, J. M. C.: Novel iodine chemistry in the marine boundary layer, *Geophys. Res. Lett.*, 31, L04112, doi:10.1029/2003GL019215, 2004.

Saiz-Lopez, A. and von Glasow, R.: Reactive halogen chemistry in the troposphere., *Chem. Soc. Rev.*, 41, 6448–6472, doi:10.1039/c2cs35208g, 2012.

Saiz-Lopez, A., Shillito, J. A., Coe, H., and Plane, J. M. C.: Measurements and modelling of I_2 , IO , OIO , BrO and NO_3 in the mid-latitude marine boundary layer, *Atmos. Chem. Phys.*, 6, 1513–1528, doi:10.5194/acp-6-1513-2006, 2006.

Saiz-Lopez, A., Mahajan, A. S., Salmon, R. A., Bauguitte, S. J.-B., Jones, A. E., Roscoe, H. K., and Plane, J. M. C.: Boundary layer halogens in coastal Antarctica, *Science*, 317, 348–351, doi:10.1126/science.1141408, 2007.

Saiz-Lopez, A., Plane, J. M. C., Mahajan, A. S., Anderson, P. S., Bauguitte, S. J.-B., Jones, A. E., Roscoe, H. K., Salmon, R. A., Bloss, W. J., Lee, J. D., and Heard, D. E.: On the vertical distribution of boundary layer halogens over coastal Antarctica: implications for O_3 , HO_x , NO_x and the Hg lifetime, *Atmos. Chem. Phys.*, 8, 887–900, doi:10.5194/acp-8-887-2008, 2008.

Saiz-Lopez, A., Plane, J. M. C., Baker, A. R., Carpenter, L. J., von Glasow, R., Martín, J. C. G., McFiggans, G., and Saunders, R. W.: Atmospheric chemistry of iodine, *Chem. Rev.*, 112, 1773–804, doi:10.1021/cr200029u, 2012a.

Saiz-Lopez, A., Lamarque, J.-F., Kinnison, D. E., Tilmes, S., Ordóñez, C., Orlando, J. J., Conley, A. J., Plane, J. M. C., Mahajan, A. S., Sousa Santos, G., Atlas, E. L., Blake, D. R., Sander, S. P., Schauffler, S., Thompson, A. M., and Brasseur, G.: Estimating the climate significance of halogen-driven ozone loss in the tropical marine troposphere, *Atmos. Chem. Phys.*, 12, 3939–3949, doi:10.5194/acp-12-3939-2012, 2012b.

Iodine chemistry in the troposphere and its effect on ozone

A. Saiz-Lopez et al.

Title Page

Abstract

Introduction

Conclusions

References

Tables

Figures



Back

Close

Full Screen / Esc

Printer-friendly Version

Interactive Discussion



Sakamoto, Y., Yabushita, A., Kawasaki, M., and Enami, S.: Direct emission of I₂ molecule and IO radical from the heterogeneous reactions of gaseous ozone with aqueous potassium iodide solution, *J. Phys. Chem. A*, 113, 7707–13, doi:10.1021/jp903486u, 2009.

Salawitch, R. J., Weisenstein, D. K., Kovalenko, L. J., Sioris, C. E., Wennberg, P. O., Chance, K., Ko, M. K. W., and McLinden, C. A.: Sensitivity of ozone to bromine in the lower stratosphere, *Geophys. Res. Lett.*, 32, L05811, doi:10.1029/2004GL021504, 2005.

Sander, R.: Compilation of Henry's Law Constants for Inorganic and Organic Species of Potential Importance in Environmental Chemistry (v3), available at: <http://www.henrys-law.org/> (last access 28 May 2014), 1999.

Sander, S. P., Friedl, R. R., Golden, D. M., Kurylo, M. J., Moortgat, G. K., Wine, P. H., Ravishankara, A. R., Kolb, C. E., Molina, M. J., Diego, S., Jolla, L., Huie, R. E., and Orkin, V. L.: Chemical Kinetics and Photochemical Data for Use in Atmospheric Studies Evaluation Number 15, JPL_NASA, 06-2(15), Jet Propulsion Laboratory, Pasadena, CA, 2006.

Sander, S. P., Friedl, R. R., Barker, J. R., Golden, D. M., Kurylo, M. J., Sciences, G. E., Wine, P. H., Abbatt, J. P. D., Burkholder, J. B., Kolb, C. E., Moortgat, G. K., Huie, R. E., and Orkin, V. L.: Chemical Kinetics and Photochemical Data for Use in Atmospheric Studies, Evaluation No. 17, JPL_NASA, 10-6(17), Jet Propulsion Laboratory, Pasadena, CA, 2011.

Saunders, R. W. and Plane, J. M. C.: Formation pathways and composition of iodine oxide ultra-fine particles, *Environ. Chem.*, 2, 299, doi:10.1071/EN05079, 2005.

Saunders, R. W., Kumar, R., Gómez Martín, J. C., Mahajan, a. S., Murray, B. J., and Plane, J. M. C.: Studies of the formation and growth of aerosol from molecular iodine precursor, *Z. Phys. Chem.*, 224, 1095–1117, doi:10.1524/zpch.2010.6143, 2010.

Solomon, S., Garcia, R. R., and Ravishankara, A. R.: On the role of iodine in ozone depletion, *J. Geophys. Res.*, 99, 20491, doi:10.1029/94JD02028, 1994.

Sommariva, R. and von Glasow, R.: Multiphase halogen chemistry in the tropical Atlantic Ocean, *Environ. Sci. Technol.*, 46, 10429–10437, doi:10.1021/es300209f, 2012.

Sommariva, R., Bloss, W. J., and von Glasow, R.: Uncertainties in gas-phase atmospheric iodine chemistry, *Atmos. Environ.*, 57, 219–232, doi:10.1016/j.atmosenv.2012.04.032, 2012.

Spietz, P., Gómez Martín, J. C., and Burrows, J. P.: Spectroscopic studies of the I₂/O₃ photochemistry Part 2. Improved spectra of iodine oxides and analysis of the IO absorption spectrum, *J. Photoch. Photobio. A*, 176, 50–67, doi:10.1016/j.jphotochem.2005.08.023, 2005.

Tegtmeier, S., Krüger, K., Quack, B., Atlas, E., Blake, D. R., Boenisch, H., Engel, A., Hepach, H., Hossaini, R., Navarro, M. A., Raimund, S., Sala, S., Shi, Q., and Ziska, F.: The contribution

of oceanic methyl iodide to stratospheric iodine, *Atmos. Chem. Phys.*, 13, 11869–11886, doi:10.5194/acp-13-11869-2013, 2013.

Vogt, R., Sander, R., Glasow, R. von and Crutzen, P. J.: Iodine chemistry and its role in halogen activation and ozone loss in the marine boundary layer: a model study, *J. Atmos. Chem.*, 32, 375–395, doi:10.1023/A:1006179901037, 1999.

Wegner, T., Kinnison, D. E., Garcia, R. R., and Solomon, S.: Simulation of polar stratospheric clouds in the specified dynamics version of the whole atmosphere community climate model, *J. Geophys. Res.-Atmos.*, 118, 4991–5002, doi:10.1002/jgrd.50415, 2013.

Young, P. J., Archibald, A. T., Bowman, K. W., Lamarque, J.-F., Naik, V., Stevenson, D. S., Tilmes, S., Voulgarakis, A., Wild, O., Bergmann, D., Cameron-Smith, P., Cionni, I., Collins, W. J., Dalsøren, S. B., Doherty, R. M., Eyring, V., Faluvegi, G., Horowitz, L. W., Josse, B., Lee, Y. H., MacKenzie, I. A., Nagashima, T., Plummer, D. A., Righi, M., Rumbold, S. T., Skeie, R. B., Shindell, D. T., Strode, S. A., Sudo, K., Szopa, S., and Zeng, G.: Pre-industrial to end 21st century projections of tropospheric ozone from the Atmospheric Chemistry and Climate Model Intercomparison Project (ACCMIP), *Atmos. Chem. Phys.*, 13, 2063–2090, doi:10.5194/acp-13-2063-2013, 2013.

Iodine chemistry in the troposphere and its effect on ozone

A. Saiz-Lopez et al.

Title Page

Abstract

Introduction

Conclusions

References

Tables

Figures



Back

Close

Full Screen / Esc

Printer-friendly Version

Interactive Discussion



Table 1. Iodine chemistry scheme in CAM-Chem: bimolecular, thermal decomposition and termolecular reactions.

Reaction	$\text{k cm}^{-3} \text{ molecule}^{-1} \text{ s}^{-1}$	Notes
$\text{I} + \text{O}_3 \rightarrow \text{IO} + \text{O}_2$	$2.1 \times 10^{-11} e^{(-830/T)}$	1
$\text{IO} + \text{O}_3 \rightarrow \text{OIO} + \text{O}_2$	3.6×10^{-16}	2
$\text{I} + \text{HO}_2 \rightarrow \text{HI} + \text{O}_2$	$1.5 \times 10^{-11} e^{(-1090/T)}$	3
$\text{IO} + \text{NO} \rightarrow \text{I} + \text{NO}_2$	$7.15 \times 10^{-12} e^{(300/T)}$	1
$\text{IO} + \text{HO}_2 \rightarrow \text{HOI} + \text{O}_2$	$1.4 \times 10^{-11} e^{(540/T)}$	1
$\text{IO} + \text{IO} \rightarrow \text{OIO} + \text{I}$	$2.13 \times 10^{-11} e^{(180/T)} \times [1 + e^{(-p/191.42)}]$	1, 4
$\text{IO} + \text{IO} (+M) \rightarrow \text{I}_2\text{O}_2 (+M)$	$3.27 \times 10^{-11} e^{(180/T)} \times [1 - 0.65e^{(-p/191.42)}]$	1, 4
$\text{IO} + \text{OIO} (+M) \rightarrow \text{I}_2\text{O}_3 (+M)$	$w_1 \times \exp(w_2 \times T)^a$	4, 5, 6 ^g
$\text{OIO} + \text{OIO} (+M) \rightarrow \text{I}_2\text{O}_4 (+M)$	$w_1 \times \exp(w_2 \times T)^b$	4, 5, 6 ^g
$\text{I}_2 + \text{O} \rightarrow \text{IO} + \text{I}$	1.25×10^{-10}	1
$\text{IO} + \text{O} \rightarrow \text{I} + \text{O}_2$	1.4×10^{-10}	1
$\text{IO} + \text{OH} \rightarrow \text{HO}_2 + \text{I}$	1.0×10^{-10}	7
$\text{I}_2\text{O}_2 (+M) \rightarrow \text{OIO} + \text{I} (+M)$	$w_1 \times \exp(w_2/T)^c$	5, 6, 8 ^g
$\text{I}_2\text{O}_2 (+M) \rightarrow \text{IO} + \text{IO} (+M)$	$w_1 \times \exp(w_2/T)^d$	5, 6, 8 ^g
$\text{I}_2\text{O}_4 (+M) \rightarrow 2\text{OIO} (+M)$	$w_1 \times \exp(w_2/T)^e$	5, 8 ^g
$\text{I}_2 + \text{OH} \rightarrow \text{HOI} + \text{I}$	1.8×10^{-10}	3
$\text{I}_2 + \text{NO}_3 \rightarrow \text{I} + \text{IONO}_2$	1.5×10^{-12}	9
$\text{I} + \text{NO}_3 \rightarrow \text{IO} + \text{NO}_2$	1.0×10^{-10}	1
$\text{OH} + \text{HI} \rightarrow \text{I} + \text{H}_2\text{O}$	$1.6 \times 10^{-11} e^{(440/T)}$	1
$\text{I} + \text{IONO}_2 \rightarrow \text{I}_2 + \text{NO}_3$	$9.1 \times 10^{-11} e^{(-146/T)}$	5
$\text{HOI} + \text{OH} \rightarrow \text{IO} + \text{H}_2\text{O}$	2.0×10^{-13}	10
$\text{IO} + \text{DMS} \rightarrow \text{DMSO} + \text{I}$	$3.2 \times 10^{-13} e^{(-925/T)}$	11
$\text{INO}_2 (+M) \rightarrow \text{I} + \text{NO}_2 (+M)$	$1008 \times 10^{15} e^{(-13670/T)}$	12, 13, 14
$\text{IONO}_2 (+M) \rightarrow \text{IO} + \text{NO}_2 (+M)$	$w_1 \times \exp(w_2/T)^f$	5, 15
$\text{INO} + \text{INO} \rightarrow \text{I}_2 + 2\text{NO}$	$8.4 \times 10^{-11} e^{(-2620/T)}$	3
$\text{INO}_2 + \text{INO}_2 \rightarrow \text{I}_2 + 2\text{NO}_2$	$4.7 \times 10^{-13} e^{(-1670/T)}$	1
$\text{OIO} + \text{NO} \rightarrow \text{IO} + \text{NO}_2$	$1.1 \times 10^{-12} e^{(542/T)}$	14
$\text{IO} + \text{NO}_3 \rightarrow \text{OIO} + \text{NO}_2$	9.0×10^{-12}	2
$\text{HI} + \text{NO}_3 \rightarrow \text{I} + \text{HNO}_3$	$1.3 \times 10^{-12} e^{(-1830/T)}$	16
$\text{IO} + \text{BrO} \rightarrow \text{Br} + \text{I} + \text{O}_2$	$0.30 \times 10^{-11} e^{(510/T)}$	1
$\text{IO} + \text{BrO} \rightarrow \text{Br} + \text{OIO}$	$1.20 \times 10^{-11} e^{(510/T)}$	1

Title Page

Abstract

Introduction

Conclusions

References

Tables

Figures

◀

▶

◀

▶

Back

Close

Full Screen / Esc

Printer-friendly Version

Interactive Discussion



Table 1. Continued.

Reaction	k cm ³ molecule ⁻¹ s ⁻¹	Notes
I + BrO → IO + Br	1.44×10^{-11}	17, 18, 19
IO + ClO → I + OClO	$2.585 \times 10^{-12} e^{(280/T)}$	1
IO + ClO → I + Cl + O ₂	$1.175 \times 10^{-12} e^{(280/T)}$	1
IO + ClO → ICl + O ₂	$0.940 \times 10^{-12} e^{(280/T)}$	1
IO + Br → I + BrO	2.49×10^{-11}	18, 19
CH ₃ I + OH → I + H ₂ O + HO ₂	$2.90 \times 10^{-12} e^{(-1100/T)}$	3
I + NO ₂ (+M) → INO ₂ (+M)	$k_0 = 3 \times 10^{-31} \times (T/300)^{-1} k_\infty = 6.6 \times 10^{-11}$	3 ^h
IO + NO ₂ (+M) → IONO ₂ (+M)	$k_0 = 6.5 \times 10^{-31} \times (T/300)^{-3.5} k_\infty = 7.6 \times 10^{-12} \times (T/300)^{-1.5}$	3 ^h
I + NO (+M) → INO(+M)	$k_0 = 1.8 \times 10^{-32} \times (T/300)^{-1} k_\infty = 1.7 \times 10^{-11}$	3 ^h

¹ IUPAC-2008 (Atkinson et al., 2007); ² Dillon et al. (2006); ³ JPL-2010 (Sander et al., 2011); ⁴ Gómez Martín et al. (2007); ⁵ Kaltsoyannis and Plane (2008); ⁶ Gálvez et al. (2013); ⁷ Bösch et al. (2003); ⁸ Gómez Martín and Plane (2009); ⁹ Chambers et al. (1992); ¹⁰ Chameides and Davis (1980); ¹¹ Dillon et al. (2008); ¹² McFiggans et al. (2000); ¹³ Jenkin et al. (1985); ¹⁴ Plane et al. (2006); ¹⁵ Allan and Plane (2002); ¹⁶ Lancar et al. (1991); ¹⁷ Laszlo et al. (1997); ¹⁸ Bedjanian et al. (1997); ¹⁹ Gilles et al. (1997).

$$a \quad w_1 = 4.687 \times 10^{-10} - 1.3855 \times 10^{-5} \times e^{(-0.75p/1.62265)} + 5.51868 \times 10^{-10} \times e^{(-0.75p/199.328)}$$

$$w_2 = -0.00331 - 0.00514 \times e^{(-0.75p/325.68711)} - 0.00444 \times e^{(-0.75p/40.81609)}$$

$$b \quad w_1 = 1.1659 \times 10^{-9} - 7.79644 \times 10^{-10} e^{(-0.75p/22.09281)} + 1.03779 \times 10^{-9} \times e^{(-0.75p/568.15381)}$$

$$w_2 = -0.00813 - 0.00382 \times e^{(-0.75p/45.57591)} - 0.00643 \times e^{(-0.75p/417.95061)}$$

$$c \quad w_1 = 3.54288 \times 10^{10} + 1.8523 \times 10^{11} \times 0.75p - 1.45435 \times 10^8 \times (0.75p)^2 + 60799.4344 \times (0.75p)^3$$

$$w_2 = -9681.65989 + 346.95538 \times e^{(-0.75p/343.25322)} + 251.78032 \times e^{(-0.75p/44.1466)}$$

$$d \quad w_1 = 255335000000 - 4418880000 \times 0.75p + 85618600 \times (0.75p)^2 + 14218.81 \times (0.75p)^3$$

$$w_2 = -11466.82304 + 597.01334 \times e^{(-0.75p/1382.62325)} - 167.3391 \times e^{(-0.75p/43.75089)}$$

$$e \quad w_1 = -1.92626 \times 10^{14} + 4.67414 \times 10^{13} \times 0.75p - 3.68651 \times 10^8 \times (0.75p)^2 - 3.09109 \times 10^6 \times (0.75p)^3$$

$$w_2 = -12302.15294 + 252.78367 \times e^{(-0.75p/46.12733)} + 437.62868 \times e^{(-0.75p/428.4413)}$$

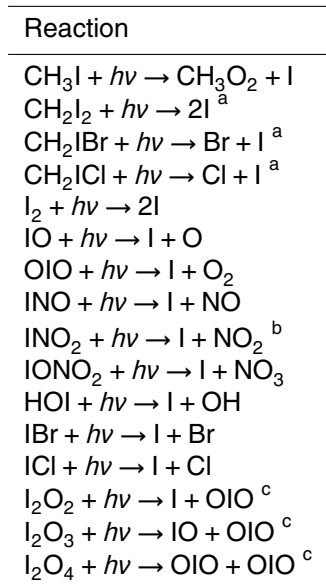
$$f \quad w_1 = -2.63544 \times 10^{13} + 4.32845 \times 10^{12} \times (0.75p) + 3.73758 \times 10^8 \times (0.75p)^2 - 628468.76313 \times (0.75p)^3$$

$$w_2 = -13847.85015 + 240.34465 \times e^{(-0.75p/49.27141)} + 451.35864 \times e^{(-0.75p/436.87605)}$$

^g The empirical expressions of the form $w_1 \times \exp(w_2 \times T)$ were obtained by non-linear least squares fitting of Rice–Ramsperger–Kassel–Marcus (RRKM) theoretical results for the indicated reaction rate constants and thermal dissociation rates in the (27–1013) hPa pressure range. RRKM calculations were carried out using the MESMER algorithm (Glowacki et al., 2012) as indicated in the corresponding references (e.g. Gálvez et al., 2013). Expression ^a produces negative values outside the range of modelled rate constants ($p < 20$ hPa), and therefore a fixed rate constant of 3×10^{-11} cm³ molecule⁻¹ s⁻¹ was assumed. Expressions ^e and ^f generate negligible dissociation rates below ~500 hPa which become negative at ~8 hPa – in this case they are set to zero below that pressure. Note that the parameterised pressure range of rate constants spans the atmospheric layer relevant for this work and beyond (see Figs. 3 and 4).

^h The temperature and pressure dependent rate constant (k) is computed based on the low pressure (k_0) and the high-pressure (k_∞) rate coefficients following JPL-2010 (Sander et al., 2011).

Table 2. Iodine chemistry scheme in CAM-Chem: photochemical reactions.



Photolysis rates are computed online from absorption cross-sections and quantum yields reported in IUPAC-2008 (Atkinson et al., 2007, 2008) and JPL-2010 (Sander et al., 2011), and the online actinic flux calculation in CAM-Chem.

^a radical organic products are not considered.

^b only the reaction channel reported in JPL 06-02 (Sander et al., 2006) is considered.

^c photolysis reactions only considered in the $J_{x\text{O}_y}$ scheme.

20024

ACPD

14, 19985–20044, 2014

Iodine chemistry in the troposphere and its effect on ozone

A. Saiz-Lopez et al.

Title Page

Abstract

Introduction

Conclusions

References

Tables

Figures

◀

▶

◀

▶

Back

Close

Full Screen / Esc

Printer-friendly Version

Interactive Discussion



Iodine chemistry in the troposphere and its effect on ozone

A. Saiz-Lopez et al.

Title Page

Abstract

Introduction

Conclusions

References

Tables

Figures



Back

Close

Full Screen / Esc

Printer-friendly Version

Interactive Discussion



Table 3. Iodine chemistry scheme in CAM-Chem: heterogeneous reactions.

Sea-salt aerosol reactions	Reactive uptake
$\text{IONO}_2 \rightarrow 0.5 \text{ IBr} + 0.5 \text{ ICl}$	$\gamma = 0.01$
$\text{INO}_2 \rightarrow 0.5 \text{ IBr} + 0.5 \text{ ICl}$	$\gamma = 0.02$
$\text{HOI} \rightarrow 0.5 \text{ IBr} + 0.5 \text{ ICl}$	$\gamma = 0.06$
$\text{I}_2\text{O}_2 \rightarrow$	$\gamma = 0.01^*$
$\text{I}_2\text{O}_3 \rightarrow$	$\gamma = 0.01^*$
$\text{I}_2\text{O}_4 \rightarrow$	$\gamma = 0.01^*$

Values based on the THAMO model (Saiz-Lopez et al., 2008) and implemented in CAM-Chem following (Ordóñez et al., 2012).

* Deposition of I_xO_y species on sea-salt aerosols has been included following the free regime approximation.

Iodine chemistry in the troposphere and its effect on ozone

A. Saiz-Lopez et al.

Title Page

Abstract

Introduction

Conclusions

References

Tables

Figures



Back

Close

Full Screen / Esc

Printer-friendly Version

Interactive Discussion



Table 4. Iodine chemistry scheme in CAM-Chem: Henry's Law constants and dry deposition velocities.

Species	k_0 (M atm ⁻¹)	Deposition velocity* (cm s ⁻¹)	Reference
IBr ^{ice}	2.4×10^1	–	1
ICl ^{ice}	1.1×10^2	–	1
HI	7.8×10^{-1}	1.0	1 ^a
HOI – ($J_{\text{I}_x\text{O}_y}/\text{Base}$)	$1.9 \times 10^3/4.5 \times 10^3$	0.75	1 ^b
IONO ₂ ^{ice}	1.0×10^6	0.75	2 ^c
INO ₂ ^{ice}	3.0×10^{-1}	0.75	1 ^d
IO	4.5×10^2	–	2
OIO	1.0×10^4	–	2
I ₂ O ₂	1.0×10^4	1.0	2
I ₂ O ₃	1.0×10^4	1.0	2
I ₂ O ₄	1.0×10^4	1.0	2

* Dry deposition velocities are based on the THAMO model (Saiz-Lopez et al., 2008).

¹ Values reported in Sander (1999).

² Values based on the THAMO model (Saiz-Lopez et al., 2008).

^a Considering a dissociation constant $K_a = 3.2 \times 10^9$ and a temperature dependent coefficient $c = 9800$ K.

^b Within the range of values given in the corresponding reference.

^c Virtually infinite solubility is represented by using a very large arbitrary number.

^d Value assumed to be equal to those of BrNO₂.

^{ice} Species for which ice-uptake is considered following Neu and Prather (2012).

[Title Page](#)
[Abstract](#)
[Introduction](#)
[Conclusions](#)
[References](#)
[Tables](#)
[Figures](#)

[Back](#)
[Close](#)
[Full Screen / Esc](#)
[Printer-friendly Version](#)
[Interactive Discussion](#)

Table 5. Odd oxygen (O_x) loss rates reactions grouped by family cycles.

Family	Reaction	ΔO_x	Odd oxygen loss ¹
O_x	$O + O_3 \rightarrow 2 \times O_2$	-2	$O_{x,loss} = 2 \times R_{O+O_3} + R_{O1D+H_2O}$
	$O(1D) + H_2O \rightarrow 2 \times OH$	-1	
HO_x	$HO_2 + O \rightarrow OH + O_2$	-2 ²	$HO_{x,loss} = 2 \times (R_{HO_2+O} + R_{HO_2+O_3})$
	$HO_2 + O_3 \rightarrow OH + 2 \times O_2$	-2 ²	
NO_x	$NO_2 + O \rightarrow NO + O_2$	-2	$NO_{x,loss} = 2 \times (R_{NO_2+O} + J_{NO_3})$
	$NO_3 + h\nu \rightarrow NO + O_2$	-2	
$ClO_x + BrO_x$	$ClO + O \rightarrow Cl + O_2$	-2	$ClO_x BrO_{x,loss} = 2 \times (R_{ClO+O} + J_{Cl_2O_2} + R_{ClO+ClO}^a + R_{ClO+ClO}^b + R_{ClO+HO_2})$
	$Cl_2O_2 + h\nu \rightarrow 2 \times Cl + O_2$	-2	
	$ClO + ClO \rightarrow Cl_2 + O_2$	-2	
	$ClO + ClO \rightarrow Cl + OClO$	-2	
	$ClO + HO_2 \rightarrow HOCl + O_2$	-2 ³	
	$BrO + O \rightarrow Br + O_2$	-2	
	$BrO + BrO \rightarrow 2 \times Br + O_2$	-2	
	$BrO + HO_2 \rightarrow HOBr + O_2$	-2 ³	
	$BrO + ClO \rightarrow Br + Cl + O_2$	-2	
	$BrO + ClO \rightarrow BrCl + O_2$	-2	
IO_x	$IO + O \rightarrow I + O_2$	-2	$IO_{x,loss} = 2 \times (R_{IO+O} + J_{OIO} + R_{IO+HO_2})$
	$OIO + h\nu \rightarrow I + O_2$	-2	
	$IO + HO_2 \rightarrow HOI + O_2$	-2 ³	
	$IO + BrO \rightarrow I + Br + O_2$	-2	$+2 \times (R_{IO+BrO}^a + R_{IO+ClO}^b + R_{IO+ClO}^c)$
	$IO + ClO \rightarrow I + Cl + O_2$	-2	
	$IO + ClO \rightarrow ICl + O_2$	-2	

$O_x = O(3P) + O(1D) + O_3 + NO_2 + 2 \times NO_3 + HNO_3 + HO_2NO_2 + 2 \times N_2O_5 + ClO + 2 \times Cl_2O_2 + 2 \times OClO + 2 \times ClONO_2 + BrO + 2 \times BrONO_2 + IO + 2 \times OIO + 2 \times IO_2 + 2 \times IO_3 + 2 \times IONO_2 + 2 \times I_2O_2 + 3 \times I_2O_3 + 4 \times I_2O_4$

¹ R_{A+B} is the reaction rate for reaction $A + B \rightarrow$ products and J_C is the photodissociation rate constant (i.e. photolysis \times concentration) for $C + h\nu \rightarrow$ products. Units are $\text{molec. cm}^{-3} \text{ s}^{-1}$.

² HO_x loss cycles represent a net change $2O_3 \rightarrow 3O_2$ ($\Delta O_x = -2$) due to reactions $OH + O \rightarrow H + O_2$ and $OH + O_3 \rightarrow HO_2 + O_2$. As O_x reactions with OH are faster than with HO_2 , only the rate determining steps (RDS) have been considered multiplied by two.

³ Reactions $XO + HO_2 \rightarrow HOX + O_2$, with $X = Cl, Br$ and I , have been computed for each family with $\Delta O_x = -2$ because the photolysis of HOX produces an additional O_x loss by the OH radical (i.e. $OH + O_3 \rightarrow HO_2 + O_2$). As these $XO + HO_2$ reaction are the rate limiting step, their loss rates have been multiplied by two.

Iodine chemistry in the troposphere and its effect on ozone

A. Saiz-Lopez et al.

Table 6. Integrated odd oxygen loss rates for each ozone depleting family within the troposphere.

Simulation	Base				J_{I,O_y}			
	MBL	FT	UT	Troposphere	MBL	FT	UT	Troposphere
Tropics								
Ozone Column (DU)	1.31	13.68	9.01	24.18	1.23	13.11	8.73	23.25
ΔO_3^{OnlyBr} (DU)	-0.10	-0.57	-0.23	-0.90	-0.19	-1.14	-0.52	-1.84
ΔO_3^{NoVSL} (DU)	-0.15	-1.01	-0.51	-1.66	-0.24	-1.58	-0.79	-2.59
Ozone Loss (DU yr ⁻¹)	111.39	505.94	36.38	666.29	117.98	520.75	42.32	692.51
O _x cycles (%)	59	54	20	53	52	50	17	49
HO _x cycles (%)	20	35	58	34	18	32	47	31
ClO _x -BrO _x (%)	3	3	11	4	3	3	9	3
IO _x cycles (%)	17	8	11	9	27	14	27	16
Mid-Latitudes								
Ozone Column (DU)	1.91	17.85	10.64	30.66	1.83	17.19	10.29	29.57
ΔO_3^{OnlyBr} (DU)	-0.09	-0.56	-0.18	-0.82	-0.17	-1.22	-0.54	-1.91
ΔO_3^{NoVSL} (DU)	-0.16	-1.22	-0.52	-1.90	-0.24	-1.88	-0.87	-2.98
Ozone Loss (DU yr ⁻¹)	73.66	351.68	29.35	471.36	75.39	358.19	33.03	483.05
O _x cycles (%)	51	42	15	42	48	40	13	40
HO _x cycles (%)	33	47	63	46	31	44	53	43
ClO _x -BrO _x (%)	4	5	14	5	4	5	12	5
IO _x cycles (%)	11	6	7	6	17	11	21	12

MBL: from the ocean surface up to ~ 900 m a.s.l. (~ 900 hPa). An ocean mask discarding grid-boxes above land was applied.

FT: from ~ 900 m (~ 900 hPa) to ~ 8.5 km (~ 350 hPa).

UT: from ~ 8.5 km (~ 350 hPa) to the model tropopause. Values above the model tropopause were not considered.

Tropics: (20° N–20° S).

Midlats: (50° N–20° N) and (20° S–50° S).

$\Delta O_3^{OnlyBr} = O_3^{Iodine} - O_3^{OnlyBr}$, where *Iodine* is either *Base* or J_{I,O_y} schemes for the left and right panels of the table, respectively,

and *OnlyBr* is an equivalent simulation considering only bromine VSL sources. Analogously $\Delta O_3^{NoVSL} = O_3^{Iodine} - O_3^{NoVSL}$, where *NoVSL* is a simulation where only long-lived bromine sources have been used (see text for details).

Title Page

Abstract

Introduction

Conclusions

References

Tables

Figures

◀

▶

◀

▶

Back

Close

Full Screen / Esc

Printer-friendly Version

Interactive Discussion



Iodine chemistry in
the troposphere and
its effect on ozone

A. Saiz-Lopez et al.

Title Page

Abstract

Introduction

Conclusions

References

Tables

Figures

◀

▶

◀

▶

Back

Close

Full Screen / Esc

Printer-friendly Version

Interactive Discussion

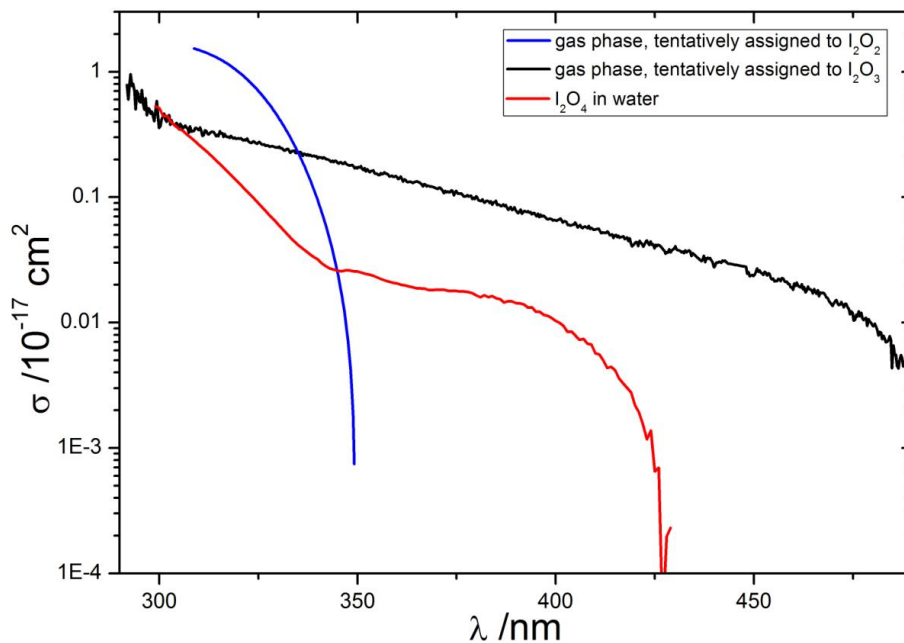


Figure 1. Absorption cross sections of the higher iodine oxides I_xO_y ($x = 2$, $y \geq 2$). Gas phase experimental spectra tentatively assigned to I_2O_2 and I_2O_3 (Gómez Martín et al., 2005, 2007; Spietz et al., 2005) are plotted in blue and black respectively. The I_2O_2 spectrum has been smoothed by fitting a polynomial through it. The red line corresponds to the absorption spectrum of I_2O_4 in water (R. Saunders, personal communication, 2011).

Iodine chemistry in the troposphere and its effect on ozone

A. Saiz-Lopez et al.

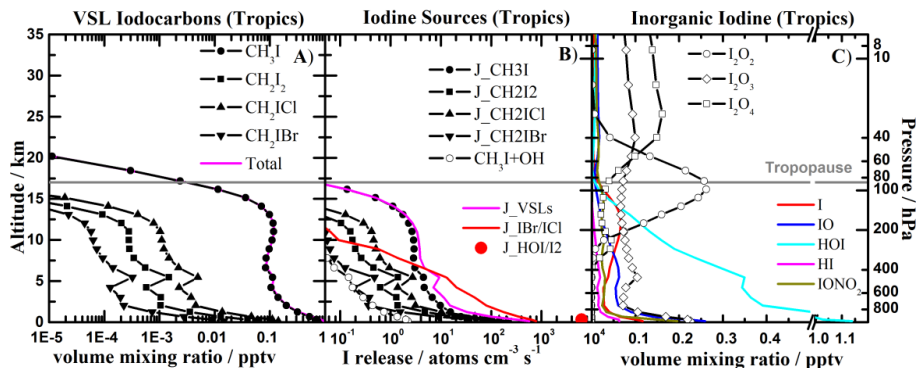


Figure 2. Vertical distributions of annually averaged organic and inorganic iodine species within the tropics (20° N–20° S): **(A)** organic VSL iodocarbons; **(B)** iodine atom released from different sources as a function of altitude, and **(C)** main I_y species for the *Base* scheme. The abundance of I_xO_y is shown by empty symbols. The horizontal line represents the approximate location of the tropical tropopause. 24 h average profiles are shown in all cases.

Title Page

Abstract

Introduction

Conclusions

References

Tables

Figures



Back

Close

Full Screen / Esc

Printer-friendly Version

Interactive Discussion



Iodine chemistry in the troposphere and its effect on ozone

A. Saiz-Lopez et al.

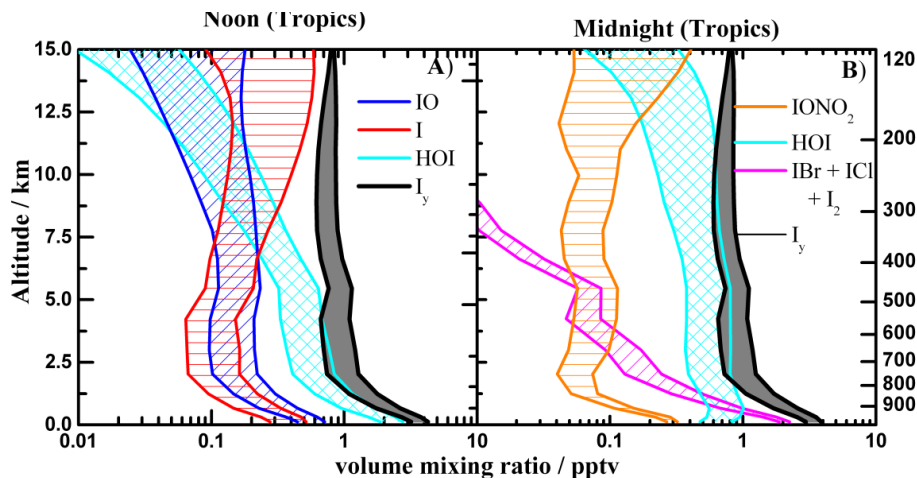


Figure 3. Lower and upper limits of I_y abundances within the tropical troposphere (20°N – 20°S): **(A)** Main inorganic species at noon; **(B)** Major I_y species at midnight. The lower limit corresponds to the *Base* scheme, while the upper limit is for the $J_{I_xO_y}$ scheme.

Title Page

Abstract

Introduction

Conclusions

References

Tables

Figures



Back

Close

Full Screen / Esc

Printer-friendly Version

Interactive Discussion



Iodine chemistry in the troposphere and its effect on ozone

A. Saiz-Lopez et al.

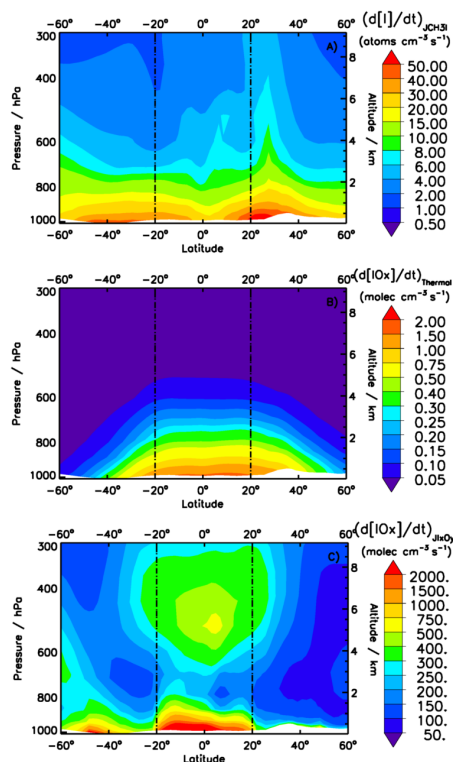


Figure 4. Annual distribution of reactive iodine ($\text{IO}_x = \text{I} + \text{IO}$) sources as a function of latitude and altitude: **(A)** atomic iodine release from photolysis of CH_3I ; **(B)** IO_x production from thermal decomposition of I_xO_y for the *Base* scheme; **(C)** Photodecomposition of higher oxides within the $J_{\text{I}_x\text{O}_y}$ scheme. Note that for **(B)** and **(C)**, the photolysis of OIO to $\text{I} + \text{O}_2$ (Gómez Martín and Plane, 2009) is so efficient that the formation of OIO from I_xO_y (Table 1) is computed here as IO_x . 24 h averages are shown in all cases.

Iodine chemistry in the troposphere and its effect on ozone

A. Saiz-Lopez et al.

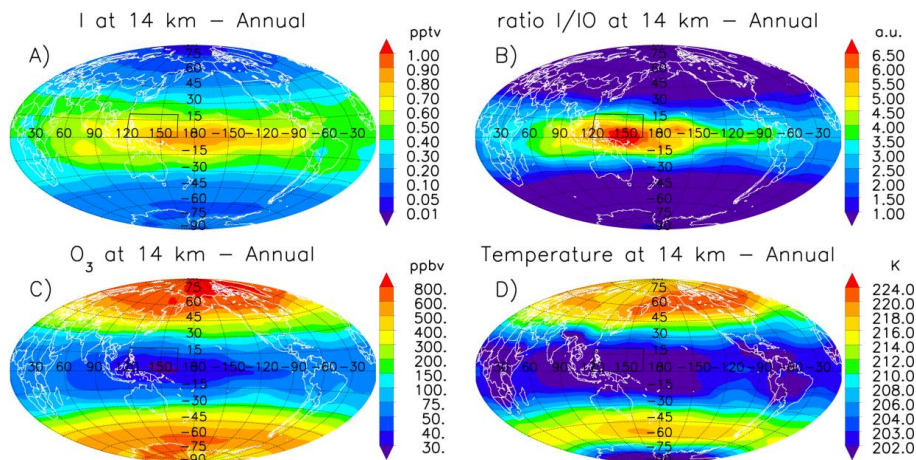


Figure 7. Average annual noontime geographical distribution at 14 km of: **(A)** atomic iodine, **(B)** I/O ratio, **(C)** ozone and **(D)** temperature. The location of the WP region, also considered to compute the vertical profiles of Fig. 6, is outlined by the black rectangle.

Title Page

Abstract

Introduction

Conclusions

References

Tables

Figures

◀

▶

◀

▶

Back

Close

Full Screen / Esc

Printer-friendly Version

Interactive Discussion



Iodine chemistry in the troposphere and its effect on ozone

A. Saiz-Lopez et al.

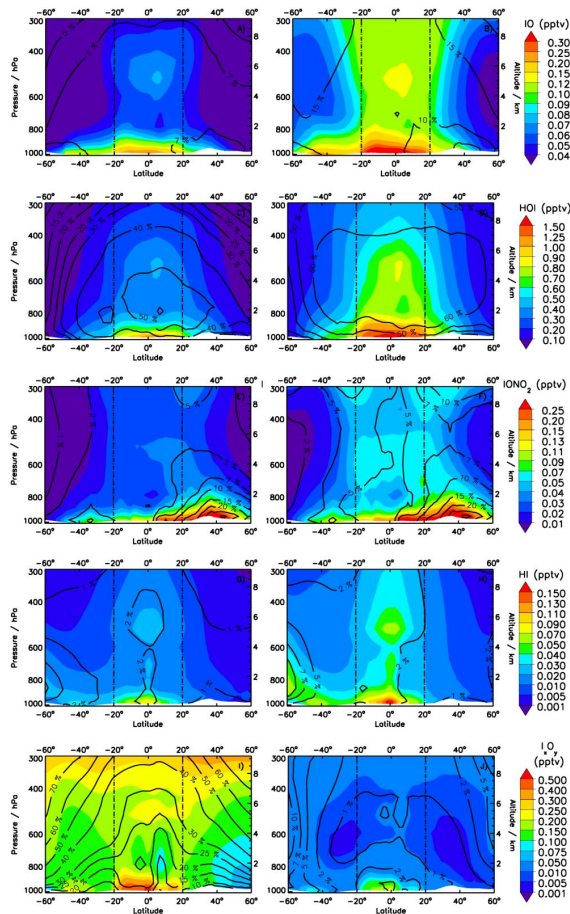


Figure 8. Annual zonal average distribution of the main I_y species in the troposphere for the *Base* (left) and $J_{I_xO_y}$ (right) schemes. The color scale represents 24 h average volume mixing ratios (pptv) while black contour lines show the percentage contribution of each species to I_y .

Iodine chemistry in the troposphere and its effect on ozone

A. Saiz-Lopez et al.

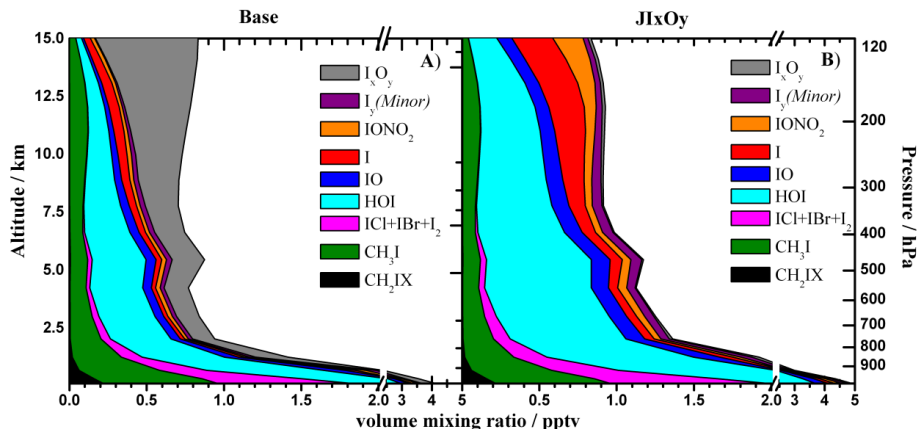


Figure 9. Annual average tropical vertical partitioning of organic and inorganic iodine for the *Base* (left) and $J_{I_xO_y}$ (right) schemes, considering both daytime and nighttime (24 h) data. Minor organic and inorganic species have been lumped together for simplicity (see text for details).

Title Page

Abstract

Introduction

Conclusions

References

Tables

Figures



Back

Close

Full Screen / Esc

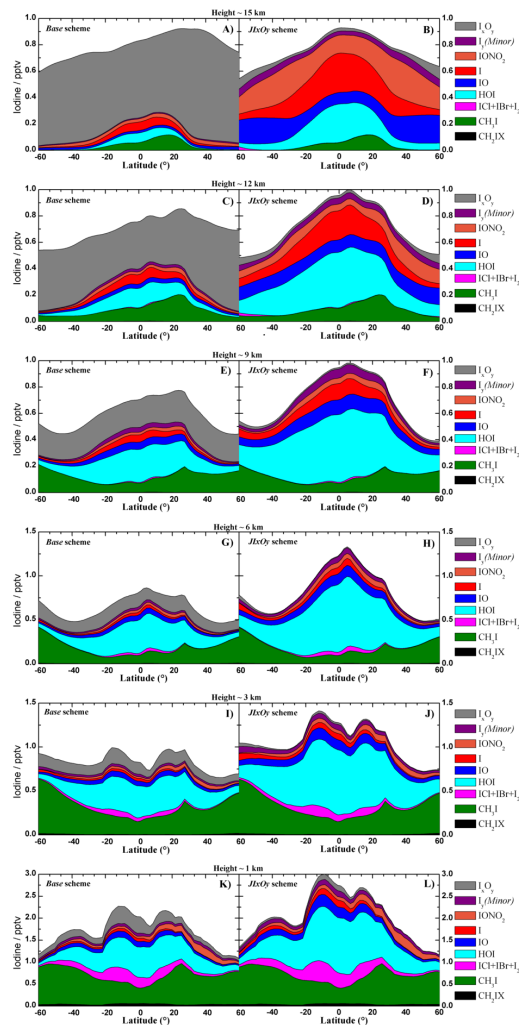
Printer-friendly Version

Interactive Discussion



Iodine chemistry in the troposphere and its effect on ozone

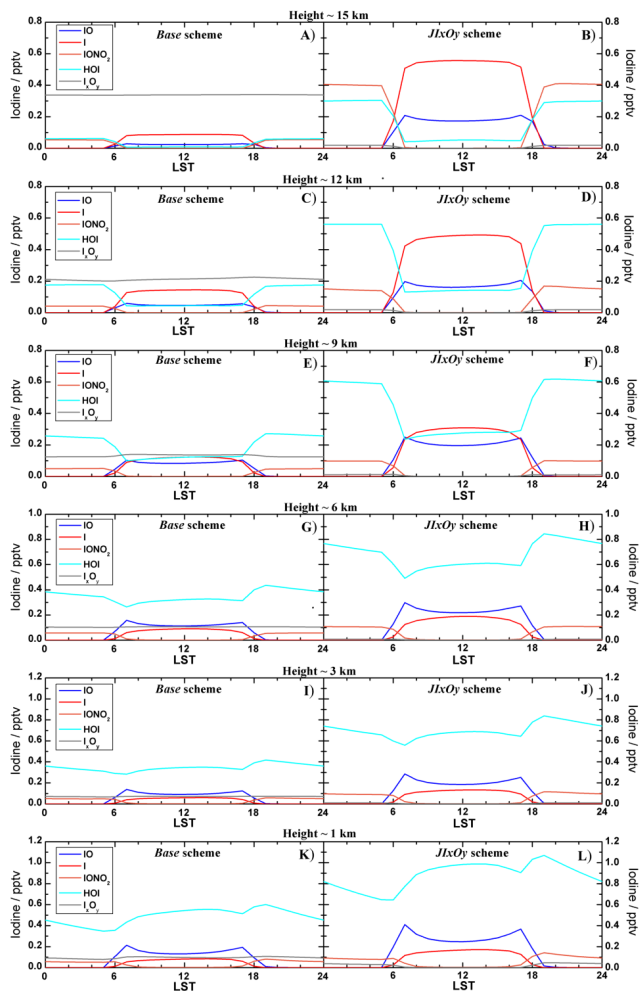
A. Saiz-Lopez et al.


[Title Page](#)
[Abstract](#)
[Introduction](#)
[Conclusions](#)
[References](#)
[Tables](#)
[Figures](#)

[Back](#)
[Close](#)
[Full Screen / Esc](#)
[Printer-friendly Version](#)
[Interactive Discussion](#)


Iodine chemistry in the troposphere and its effect on ozone

A. Saiz-Lopez et al.



[Title Page](#)

[Abstract](#)

[Introduction](#)

[Conclusions](#)

[References](#)

[Tables](#)

[Figures](#)

◀

▶

◀

▶

[Back](#)

[Close](#)

[Full Screen / Esc](#)

[Printer-friendly Version](#)

[Interactive Discussion](#)



Figure 11. Diurnal variation of main inorganic iodine species at different altitudes for the *Base* (left) and $J_{\text{I}_x\text{O}_y}$ (right) schemes. Tropical averages considering locations with equivalent local times have been computed. Results are shown at approximate heights of 1, 3, 6, 9, 12 and 15 km.

Iodine chemistry in the troposphere and its effect on ozone

A. Saiz-Lopez et al.

[Title Page](#)[Abstract](#)[Introduction](#)[Conclusions](#)[References](#)[Tables](#)[Figures](#)[Back](#)[Close](#)[Full Screen / Esc](#)[Printer-friendly Version](#)[Interactive Discussion](#)

Iodine chemistry in the troposphere and its effect on ozone

A. Saiz-Lopez et al.

Title Page

Abstract

Introduction

Conclusions

References

Tables

Figures



Back

Close

Full Screen / Esc

Printer-friendly Version

Interactive Discussion

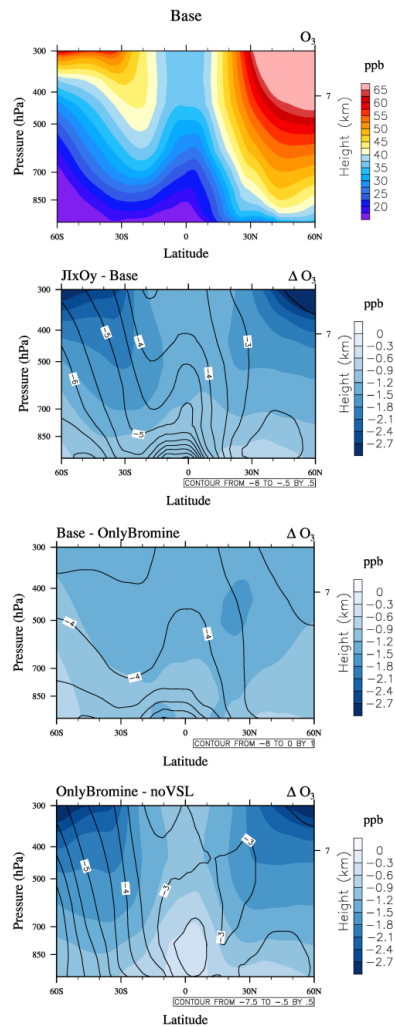


Figure 12. Zonal annual average distributions of tropospheric ozone changes for different model schemes considering iodine and bromine VSL sources: **(A)** O_3 vmr for the *Base* scheme (lower iodine loading); **(B)** difference between the higher and lower iodine schemes $\Delta O_3(J_{I,O_y} - Base)$; **(C)** impact of lower iodine respect to bromine chemistry $\Delta O_3(Base - OnlyBr)$; **(D)** impact of considering only bromine chemistry relative to only long-lived sources $\Delta O_3(OnlyBr - NoVSL)$. The colour scale represents 24 h mean model differences in ppbv, while the black contour lines show the percentage change between each pair of simulations computed as $(A - B)/B \times 100\%$.

Iodine chemistry in the troposphere and its effect on ozone

A. Saiz-Lopez et al.

[Title Page](#)[Abstract](#)[Introduction](#)[Conclusions](#)[References](#)[Tables](#)[Figures](#)[Back](#)[Close](#)[Full Screen / Esc](#)[Printer-friendly Version](#)[Interactive Discussion](#)

Iodine chemistry in the troposphere and its effect on ozone

A. Saiz-Lopez et al.

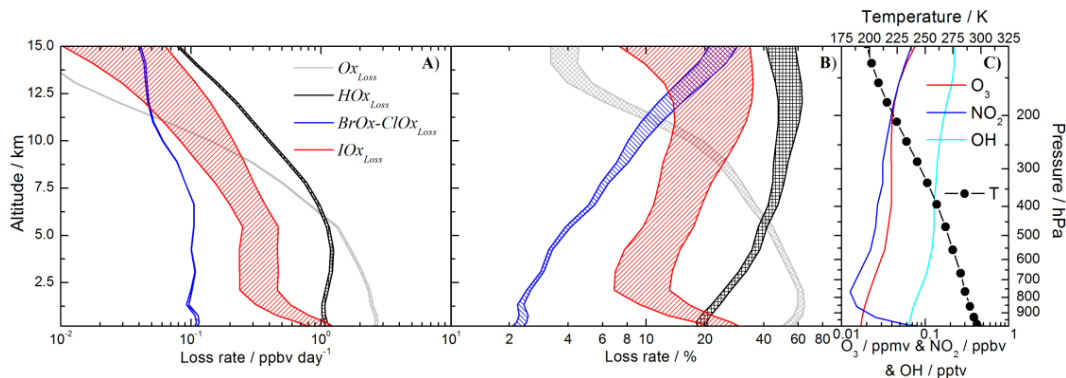


Figure 13. Modeled range of odd oxygen destruction for each of the ozone depleting families: **(A)** annual total loss rates for the O_x , HO_x , BrO_x-ClO_x and IO_x families within the tropical troposphere (20° N–20° S); **(B)** percentage contribution of each family to the total loss rate for each scheme; **(C)** vertical profiles of O_3 , NO_2 , OH and temperature within the tropics. Lower and upper limits of the range are for the *Base* and J_{xO_y} schemes, respectively.